Prof. John O. Prior, PhD MD
Nuclear Medicine and Molecular Imaging
Lausanne University Hospital, Switzerland

Practical radioprotection issues in nuclear medicine at the era of digital PET/ SPECT cameras

UNIL | Université de Lausanne

Part 1

Digital SiPM-based PET/CT Technology

PET: 3 major improvements last 3 decades

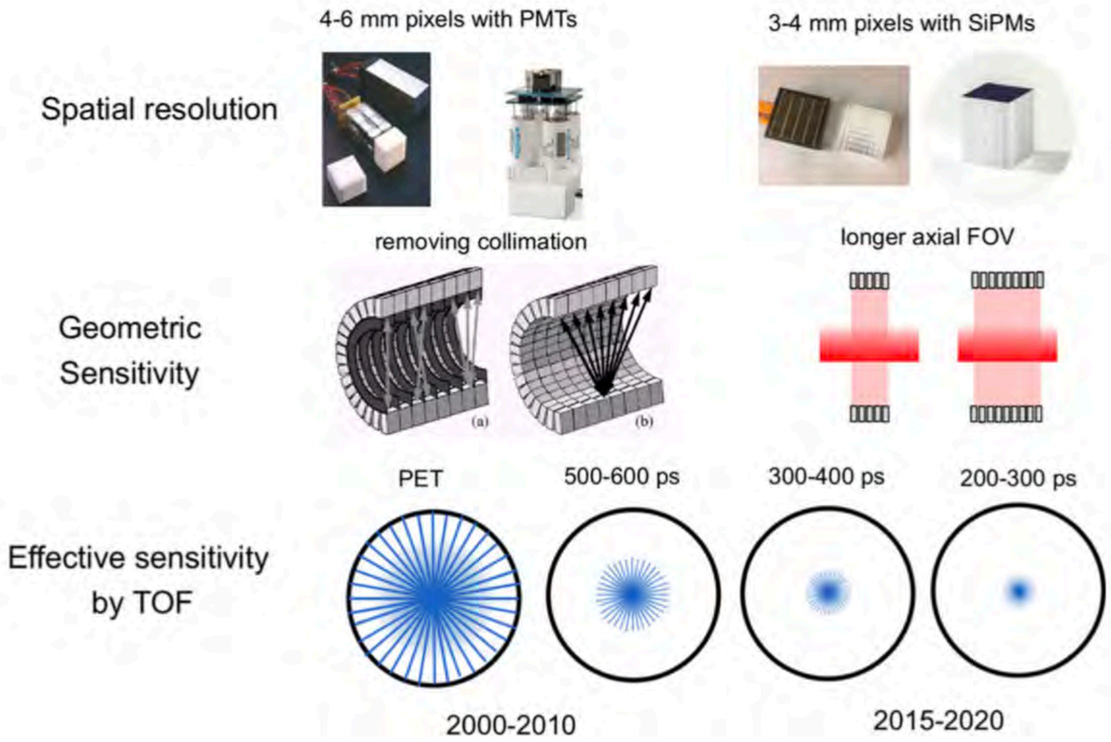

Vandenbergh EJNMMI Physics 2020;7:35

Digital SiPM PET vs. Conventional PMT PET

ORIGINAL RESEARCH — Open Access

Phantom-based image quality assessment of clinical ^{18}F-FDG protocols in digital PET/CT and comparison to conventional PMT-based PET/CT

Silvano Gnesin[1], Christine Kieffer[1], Konstantinos Zeimpekis[2], Jean-Pierre Papazyan[3], Renaud Guignard[4], John O. Prior[5], Francis R. Verdun[1] and Thiago V. M. Lima[1,6]

- 3 digital SiPM+2 convent. PMT PET
- FDG clinical oncologic protocols
- Evaluate trade-off between patient administered activity (*patient dose/signal-to-noise S/N ratio*) vs. acquisition time (*patient comfort*)

- List-mode reconstructions NEMA NU2 phantom (5 kBq/mL in background, 25 kBq/mL in spheres) for 10, 30, 90, 120, 180 & 300 s with 1–10 iterations
- Background coefficient of variation (COV)
- Spheres recovery coefficients (RCs)
- Using Time-activity-product (TAP) = scan time/bed position × mass-activity administered (min·MBq/kg)

Gnesin et al. EJNMMI 2019;7:1

Digital SiPM PET vs. Conventional PMT PET

3 different manufacturer:

- 2 PMT-based PET
- 3 digital PET

Installed in 2017-2018

(2 new manufacturer of SiPM PET/CT scanners in 2019, not included in this study)

Clinical FDG oncologic PET reconstructions protocols

Different matrix and pixel sizes

Gnesin et al. EJNMMI 2019;7:1

Table 1 Systems, acquisition and reconstruction parameters applied in clinical whole-body oncologic ^{18}F-FDG PET procedures

	Philips Vereos[d]	Siemens Vision[d]	Siemens mCT	GE Discovery-MI[d,a]	GE Discovery 690
System parameters	dPET	dPET	cPET	dPET	cPET
Axial ring extent (mm)	164	261	221	250	153
Energy window (keV)	450–613	435–585	435–650	425–650	425–650
TOF's resolution (ps)	316	215	540	370	544.3
NEMA System sensitivity (kcps/MBq)	5.6	16.4	9.6	22	7.5
Acquistion parameters					
Acq. Time (min)	1.5	2	2.5	2.5	1.5
Admin. Activity (MBq/kg)	2	2	5	1.5	3.5
Acq. Time (min) × A admin. (TAP in min × MBq/kg)	3	4	12.5	3.75	5.25
Reconstruction parameters					
Reconstruction methods	OSEM 3D TOF + PSF	OSEM 3D TOF + PSF	OSEM 3D TOF + PSF	OSEM 3D TOF + PSF	OSEM 3D TOF + PSF
Iterations and subsets (it,ss)	(3,15)/(2,10)	(4,5)	(3,21)	(3,16)	(3,16)
Filtre Gauss FWHM (mm)	0	0	3	6.4	5
Matrix size	144 × 144/ 288 × 288	440 × 440	512 × 512	256 × 256	256 × 256
Pixel size (mm)	4 × 4/2 × 2	1.65 × 1.65	1.59 × 1.59	2.73 × 2.73	2.73 × 2.73
Slice thickness (mm)	4/2	2	5	2.79	3.27

[a]In addition to OSEM, clinic FDG PET protocol for the GE Discovery MI also make use of the Q.Clear reconstruction algorithm (Q-param = 400)

[d]Digital PET systems

Digital SiPM PET vs. Conventional PMT PET

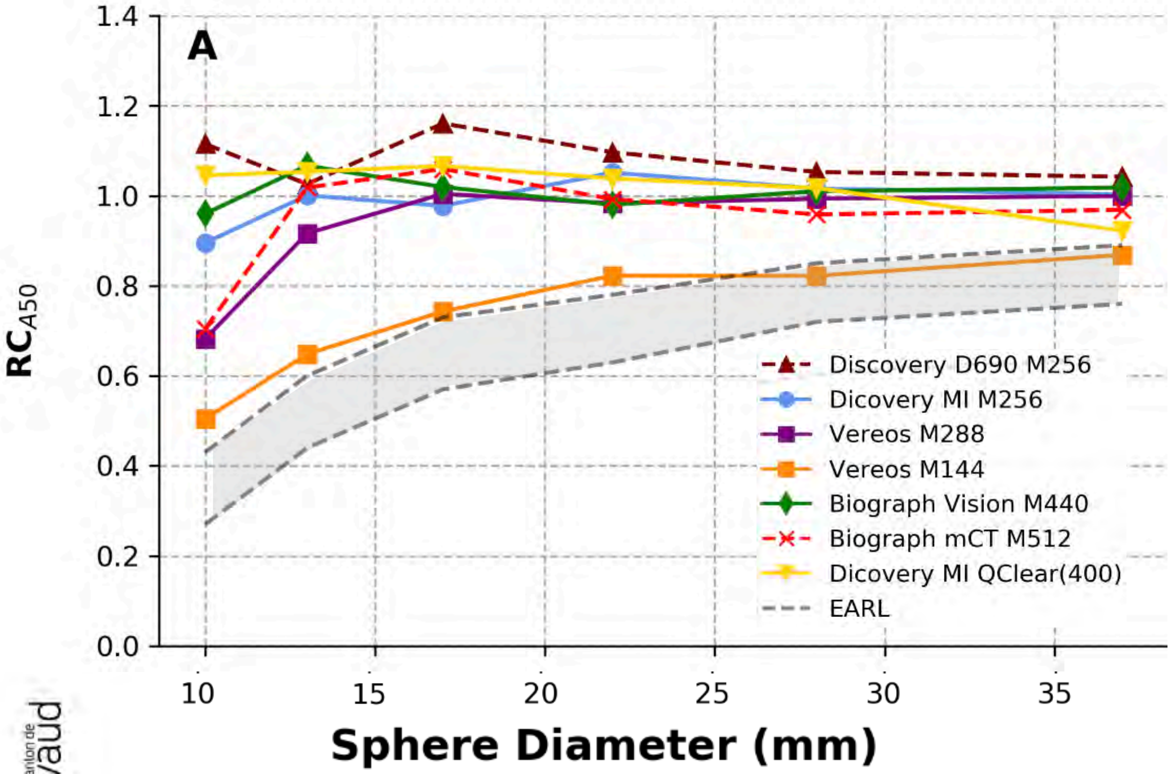

→RC comparable between digital and PMT-based PET

→EARL (2017) surpassed by most recent PET/CT systems

Gnesin et al. EJNMMI 2019;7:1

Digital SiPM PET vs. Conventional PMT PET

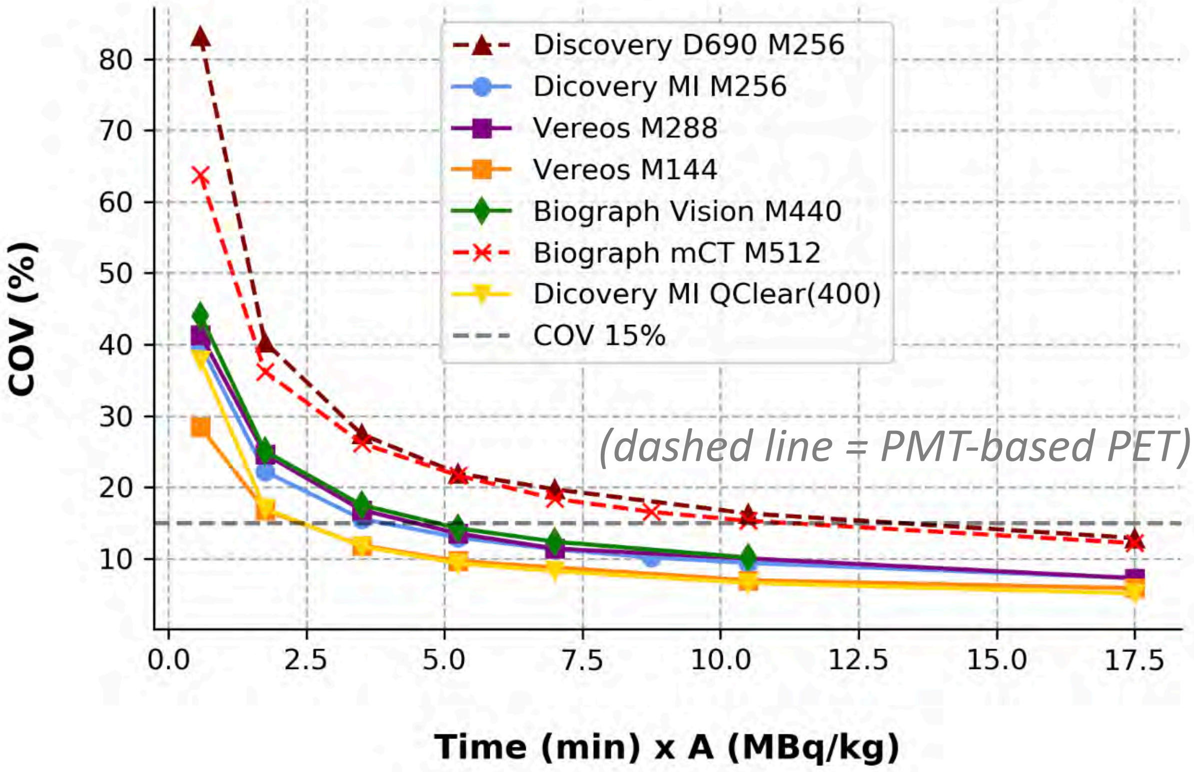

(dashed line = PMT-based PET)

→Compared to PMT-based PET, digital systems have comparable image quality for lower TAP (–40% to –70%)

Gnesin et al. EJNMMI 2019;7:1

Digital SiPM PET vs. Conventional PMT PET

Conclusions

- Image quality was comparable with a TAP reduction of >40% in digital PET
- Leads to significant reduction in mass activity or time with direct benefit for patient dose exposure and comfort

Gnesin et al. EJNMMI 2019;7:1

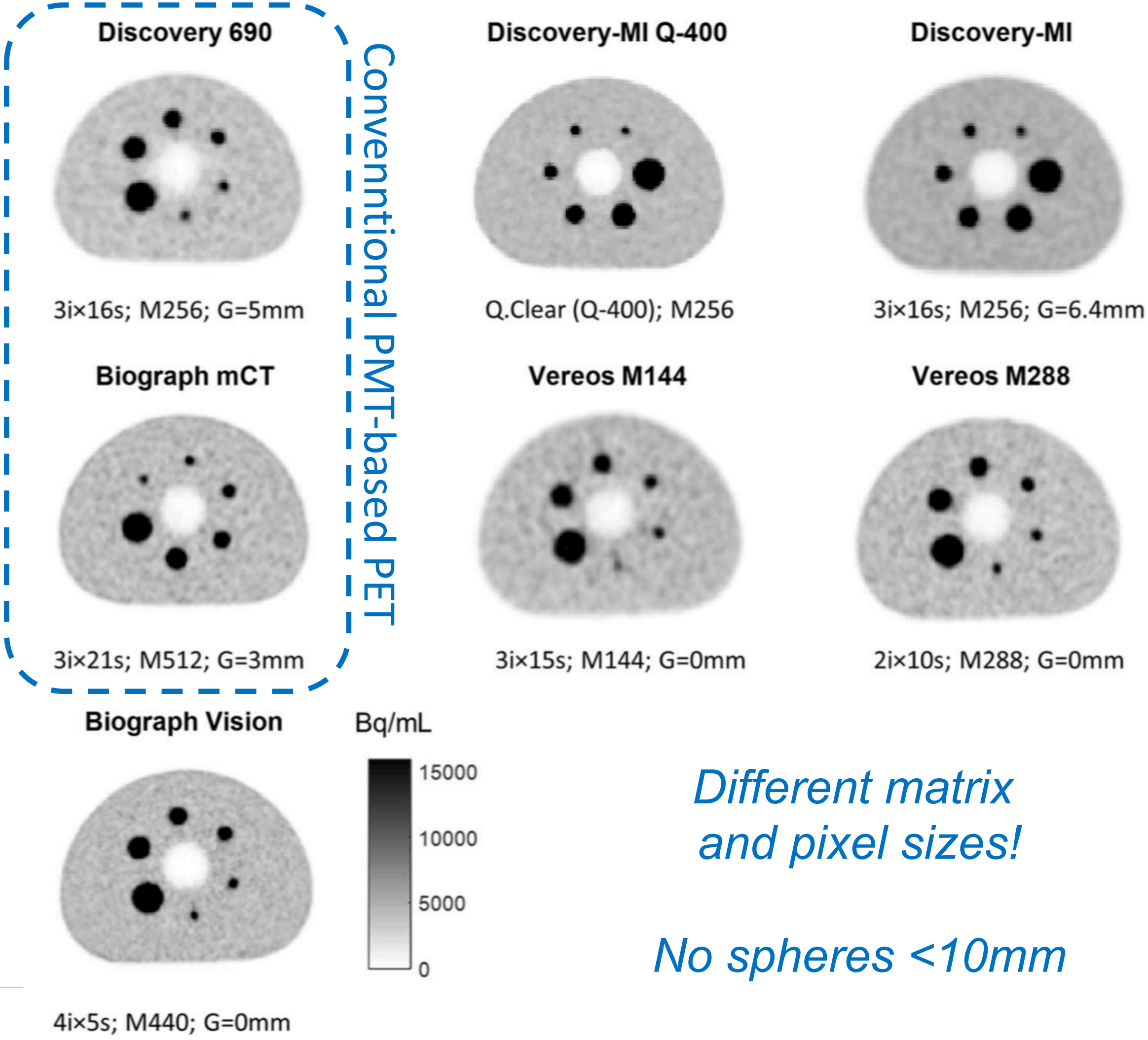

Different matrix and pixel sizes!

No spheres <10mm

2nd Worldwide installation in June 2018, N>5000 patients as of today

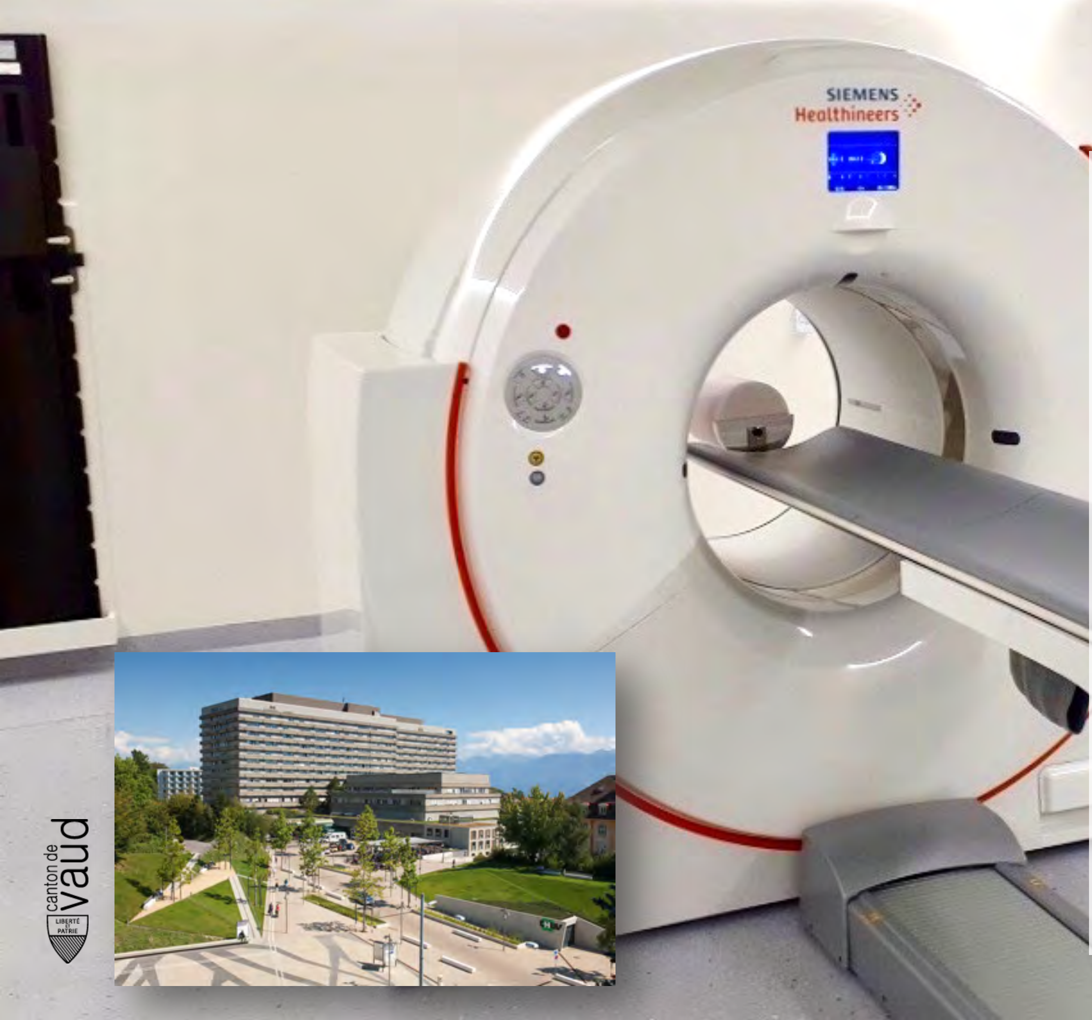

Prof. Dr. Dr. John Prior
Lausanne University Hospital

Initial Clinical Experience Digital SiPM-based PET/CT

canton de vaud
UNIL | Université de Lausanne
CHUV

First patient in Lausanne (June 2018)

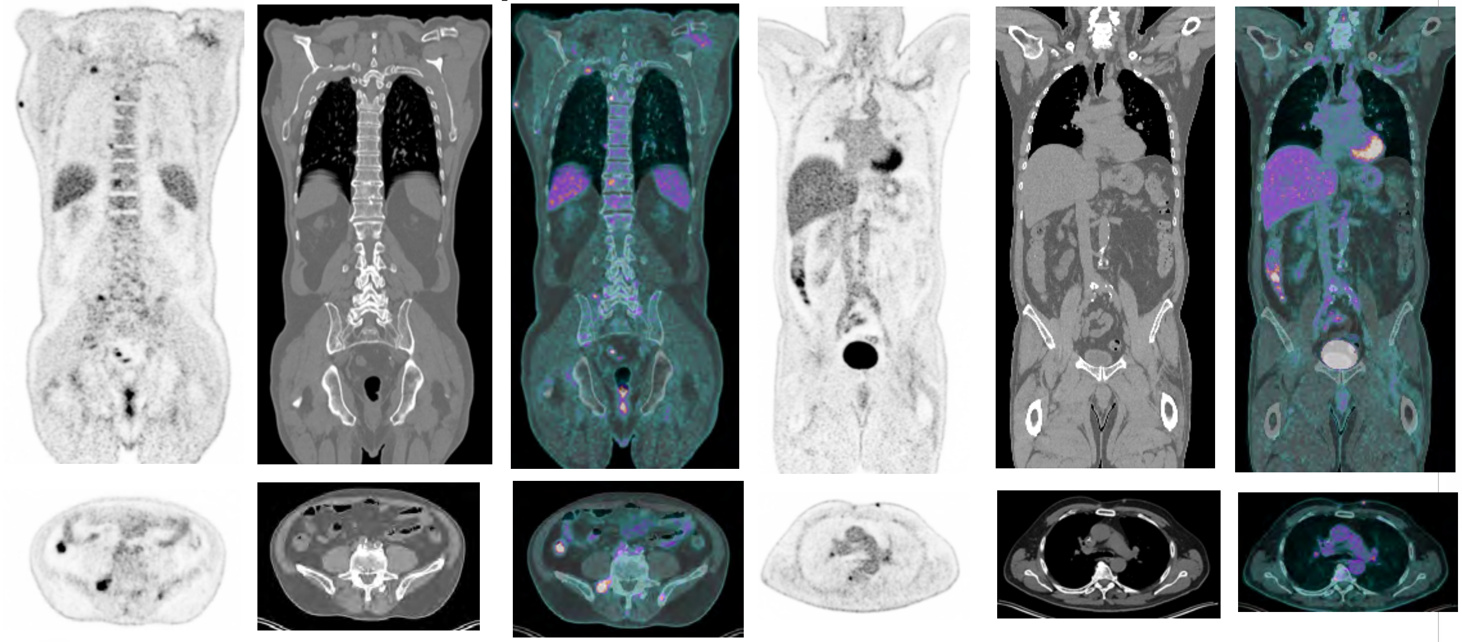

PET | CT | PET/CT fusion | PET | CT | PET/CT fusion

Today's Challenge in Oncologic Imaging

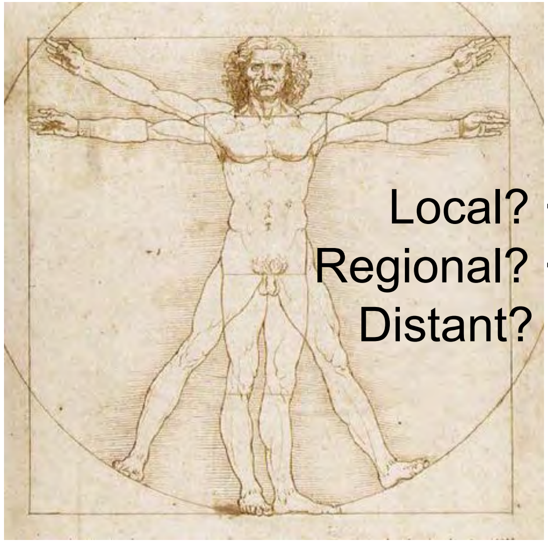

Local? → Surgery?
Regional? → Radiation?
Distant? → Chemo?

Identify all lesions is key to defining right therapy

- Local?
- Lymph nodes?
- Metastases?

Poor spatial resolution and sensitivity negatively affects lesion detectability and staging

55-y uveal melanoma patient

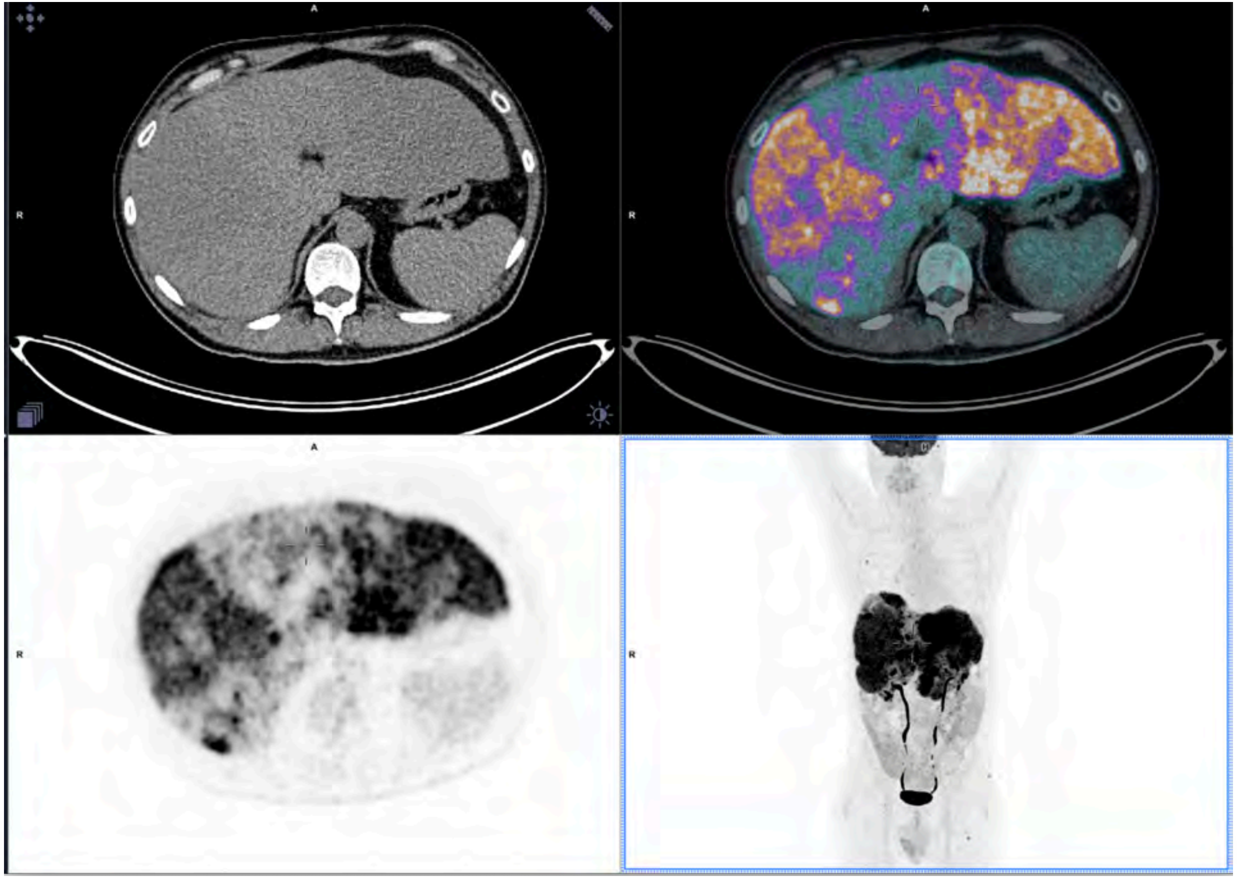

Extensive liver metastases

55-y uveal melanoma patient

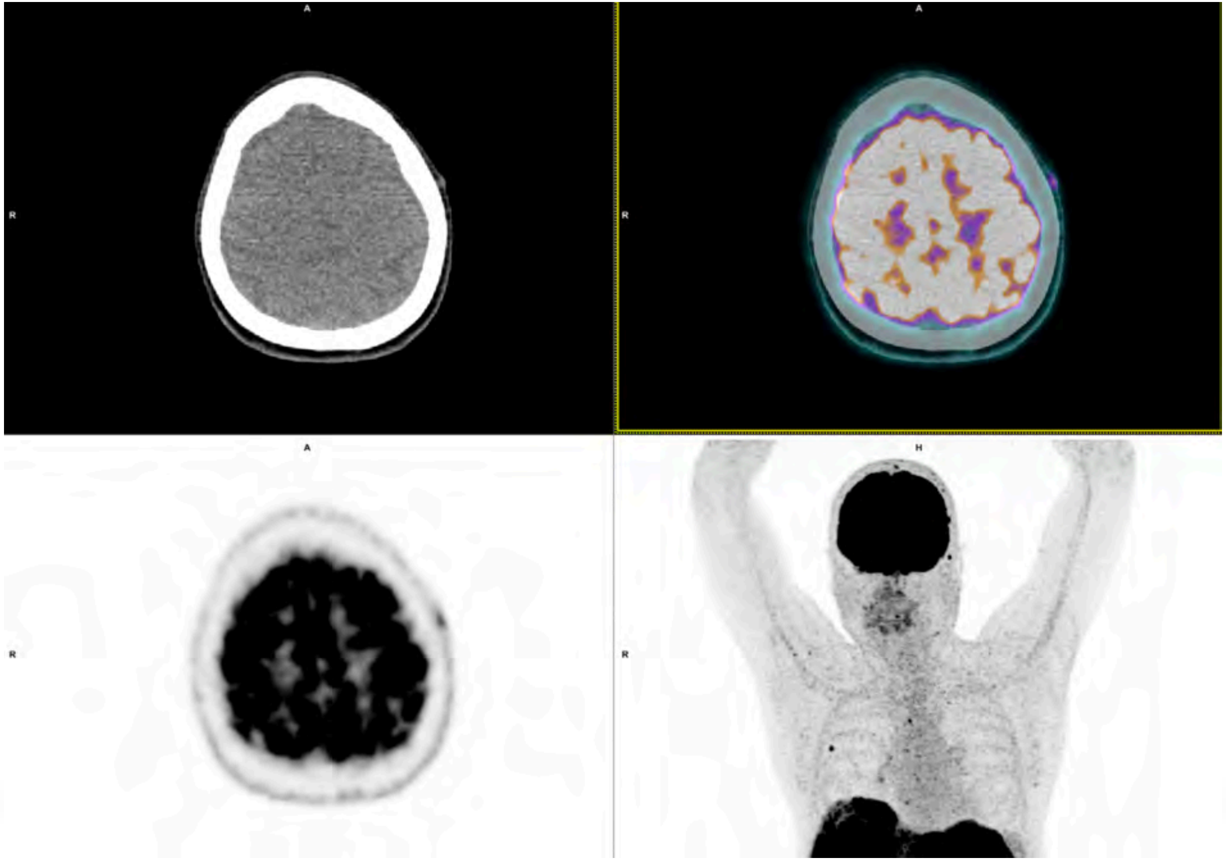

canton de vaud

Detectability of small structures in FDG PET/CT

Visual observations of the pituitary gland

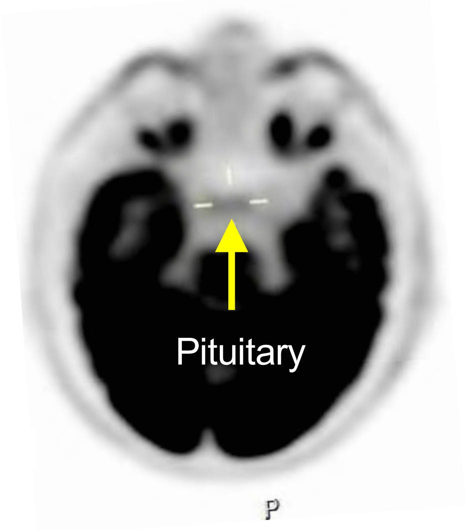

Non-Si-PM PET/CT
Gauss filter FWHM = 5mm
Voxel size : 2.74×2.74×3.27 mm

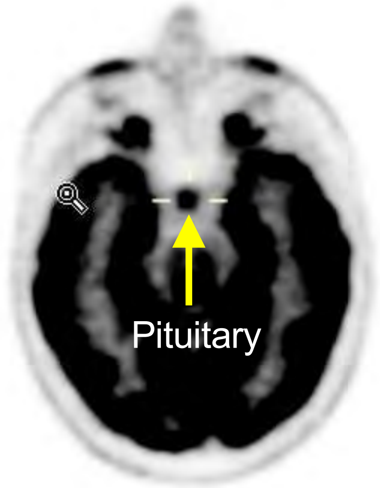

SiPM PET/CT
No gaussian Filter
Voxel size: : 1.65×1.65×2mm
→**Reduced partial volume effect**

canton de vaud

Unil UNIL | Université de Lausanne

CHUV

Increased signal recovery from small structures

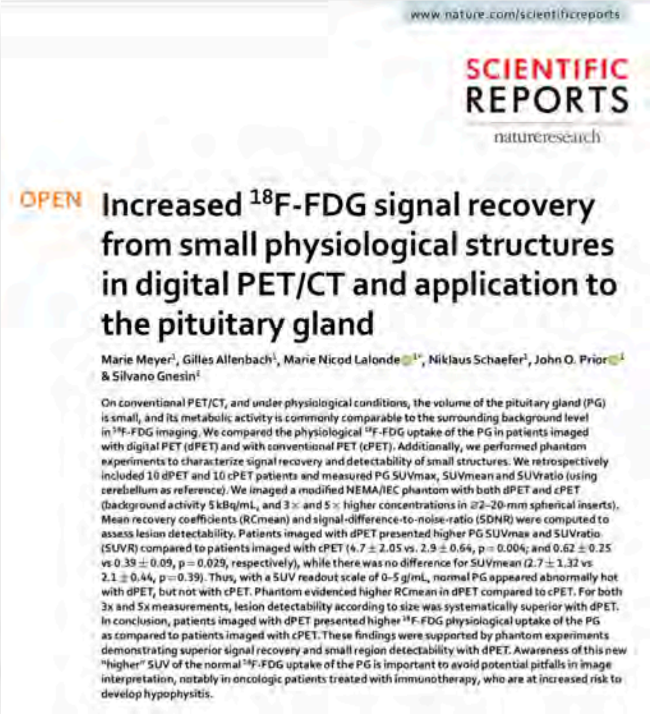
www.nature.com/scientificreports

SCIENTIFIC REPORTS

natureresearch

OPEN

Increased ^{18}F-FDG signal recovery from small physiological structures in digital PET/CT and application to the pituitary gland

Marie Meyer[1], Gilles Allenbach[1], Marie Nicod Lalonde[1*], Niklaus Schaefer[1], John O. Prior[1] & Silvano Gnesin[2]

On conventional PET/CT, and under physiological conditions, the volume of the pituitary gland (PG) is small, and its metabolic activity is commonly comparable to the surrounding background level in ^{18}F-FDG imaging. We compared the physiological ^{18}F-FDG uptake of the PG in patients imaged with digital PET (dPET) and with conventional PET (cPET). Additionally, we performed phantom experiments to characterize signal recovery and detectability of small structures. We retrospectively included 10 dPET and 10 cPET patients and measured PG SUVmax, SUVmean and SUVratio (using cerebellum as reference). We imaged a modified NEMA/IEC phantom with both dPET and cPET (background activity 5 kBq/mL, and 3 × and 5 × higher concentrations in ⌀2–20-mm spherical inserts). Mean recovery coefficients (RCmean) and signal-difference-to-noise-ratio (SDNR) were computed to assess lesion detectability. Patients imaged with dPET presented higher PG SUVmax and SUVratio (SUVR) compared to patients imaged with cPET (4.7 ± 2.05 vs. 2.9 ± 0.64, $p = 0.004$; and 0.62 ± 0.25 vs 0.39 ± 0.09, $p = 0.029$, respectively), while there was no difference for SUVmean (2.7 ± 1.32 vs 2.1 ± 0.44, $p = 0.39$). Thus, with a SUV readout scale of 0–5 g/mL, normal PG appeared abnormally hot with dPET, but not with cPET. Phantom evidenced higher RCmean in dPET compared to cPET. For both 3x and 5x measurements, lesion detectability according to size was systematically superior with dPET. In conclusion, patients imaged with dPET presented higher ^{18}F-FDG physiological uptake of the PG as compared to patients imaged with cPET. These findings were supported by phantom experiments demonstrating superior signal recovery and small region detectability with dPET. Awareness of this new "higher" SUV of the normal ^{18}F-FDG uptake of the PG is important to avoid potential pitfalls in image interpretation, notably in oncologic patients treated with immunotherapy, who are at increased risk to develop hypophysitis.

- Comparison of physiological uptake of a small structure — the pituitary gland (PG) — on dPET and cPET
- Modified NEMA/IEC phantom study with ⌀20-, 10-, 7-, 5-, 3- and 2-mm hot spheres
- 3x and 5x higher sphere activity than background concentration
- Acquisition times 1, 2, 3, 5 min
- N=10 patients each in dPET & cPET with measured SUV_{max}, SUV_{mean}, and PG volume

Meyer et al. Sci Reports 2020

Increased signal recovery from small structures

5x higher activity in spheres vs. background

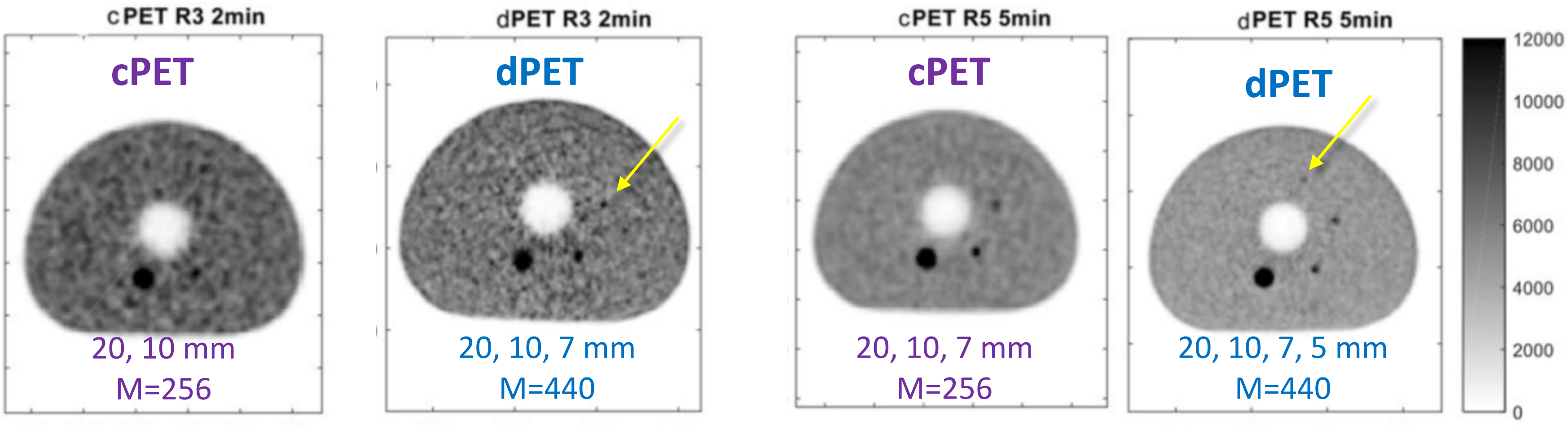

Spheres ⌀20, 10, 7, 5, 3, and 2 mm

→Superior signal recovery and small region detectability with dPET

Meyer et al. Sci Reports 2020

Increased signal recovery from small structures

3x higher activity in spheres vs. background

3x	1 min		2 min		3min		5min	
Sphere	cPET	dPET	cPET	dPET	cPET	dPET	cPET	dPET
20 mm	7.62	7.42	10.33	10.11	13.18	11.95	16.9	15.76
10 mm	2.82	3.68	3.13	5.04	4.05	6.36	5.4	8.15
7 mm	1.2	1.49	1.15	2.7	1.74	3.09	1.97	3.03

5x higher activity in spheres vs. background

5x	1 min		2 min		3min		5min	
Sphere	cPET	dPET	cPET	dPET	cPET	dPET	cPET	dPET
20 mm	17.55	16.02	23.74	22.25	28.38	27.41	35.67	35.5
10 mm	8.63	10.9	12.09	15.08	12.85	18.2	15.77	23.74
7 mm	5.03	3.33	4.81	5.65	6.04	8.49	6.69	12.34
5 mm	-0.02	4.05	0.5	3.55	0.35	4.37	0.56	4.68

Signal difference to noise ratio: SDNR >3 for detection (according to EARL 2017)

Meyer et al. Sci Reports 2020

Increased signal recovery from small structures

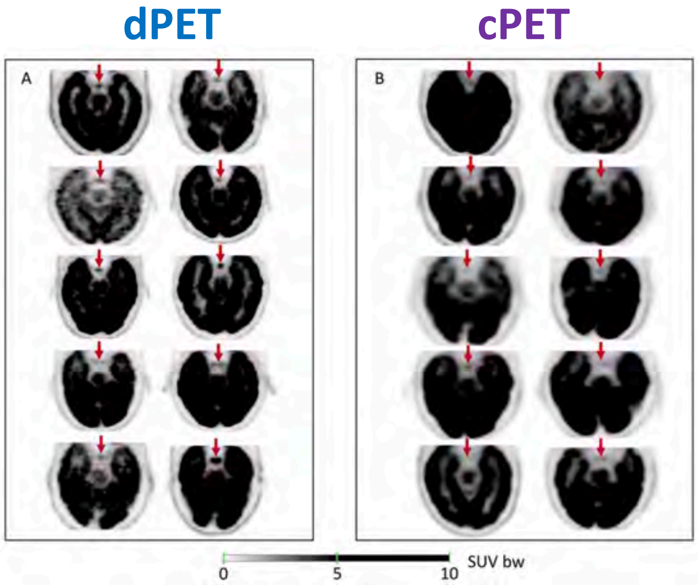

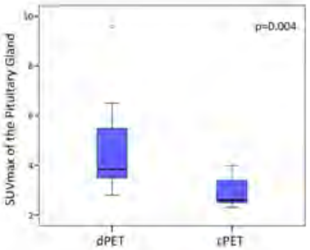

Conclusions:

→Awareness of "higher" SUV of normal pituitary FDG uptake is important to avoid potential pitfalls in interpretation

→Of importance in oncologic patients under immunotherapy, who are at increased risk to develop hypophysitis (PG inflammation)

Meyer et al. Sci Reports 2020

Lesion Detectability with Digital PET

European Journal of Nuclear Medicine and Molecular Imaging (2019) 46:1383–1390
https://doi.org/10.1007/s00259-019-4260-z

ORIGINAL ARTICLE

Comparison of image quality and lesion detection between digital and analog PET/CT

Diego Alfonso López-Mora[1] · Albert Flotats[1] · Francisco Fuentes-Ocampo[1] · Valle Camacho[1] · Alejandro Fernández[1] · Agustí Ruiz[2] · Joan Duch[1] · Marina Sizova[1] · Anna Domènech[1] · Montserrat Estorch[1] · Ignasi Carrió[1]

Received: 14 November 2018 / Accepted: 2 January 2019 / Published online: 10 January 2019

Abstract

Objective The purpose of this study was to compare image quality and lesion detection capability between a digital and an analog PET/CT system in oncological patients.

Materials and methods One hundred oncological patients (62 men, 38 women; mean age of 65 ± 12 years) were prospectively included from January–June 2018. All patients, who accepted to be scanned by two systems, consecutively underwent a single day, dual imaging protocol (digital and analog PET/CT). Three nuclear medicine physicians evaluated image quality using a 4-point scale (−1, poor; 0, fair; 1, good; 2, excellent) and detection capability by counting the number of lesions with increased radiotracer uptake. Differences were considered significant for a p value <0.05.

Results Improved image quality in the digital over the analog system was observed in 54% of the patients ($p = 0.05$, 95% CI, 44.2–63.5). The percentage of interrater concordance in lesion detection capability between the digital and analog systems was 97%, with an interrater measure agreement of $\kappa = 0.901$ ($p < 0.0001$). Although there was no significant difference in the total number of lesions detected by the two systems (digital: 5.03 ± 10.6 vs. analog: 4.53 ± 10.29; $p = 0.7$), the digital system detected more lesions in 22 of 83 of PET+ patients (26.5%) ($p = 0.05$, 95% CI, 17.9–36.7). In these 22 patients, all lesions detected by the digital PET/CT (and not by the analog PET/CT) were < 10 mm.

Conclusion Digital PET/CT offers improved image quality and lesion detection capability over the analog PET/CT in oncological patients, and even better for sub-centimeter lesions.

Keywords Digital PET/CT · Analog PET/CT · Lesion detection capability · Image quality

N=100 oncological patients

Comparison dPET vs. cPET

Improved image quality in 54 patients

dPET detected more lesions in 22 patients, all <10mm

dPET changed staging in 32% of these 22 patients

Lopez-Mora et al, EJNMMI 2019

canton de vaud

Unil | Université de Lausanne

CHUV

CHUV: HF Pulsatile Flow Ventilation Apnea PET/CT

Reduction of Respiratory Motion During PET/CT by Pulsatile-Flow Ventilation: A First Clinical Evaluation

John O. Prior*[1], Nicolas Péguret*[2], Anastasia Pomoni[1], Martin Pappon[1], Michele Zeverino[3], Bastien Belmondo[4], Alban Lovis[5], Mahmut Ozsahin[2], Monique Vienne[6], and Jean Bourhis[2]

[1]Department of Nuclear Medicine and Molecular Imaging, Lausanne University Hospital, Lausanne, Switzerland; [2]Department of Radiation Oncology, Lausanne University Hospital, Lausanne, Switzerland; [3]Department of Medical Physics, Lausanne University Hospital, Lausanne, Switzerland; [4]Department of Physiotherapy, Lausanne University Hospital, Lausanne, Switzerland; [5]Department of Pneumology, Lausanne University Hospital, Lausanne, Switzerland; and [6]BIRD Institute of Pulmonary Care, Villeneuve-Loubet, France

Respiratory motion negatively affects PET/CT image quality and quantitation. A novel Pulsatile-Flow Ventilation (PFV) system reducing respiratory motion was applied in spontaneously breathing patients to induce sustained apnea during PET/CT. **Methods:** Four patients (aged 65 ± 14 y) underwent PET/CT for pulmonary nodule staging (mean, 11 ± 7 mm; range, 5–18 mm) at 63 ± 3 min after ^{18}F-FDG injection and then at 47 ± 7 min afterward, during PFV-induced apnea (with imaging lasting ≥8.5 min). Anterior-posterior thoracic amplitude, SUV_{max}, and SUV_{peak} (SUV_{mean} in a 1-cm-diameter sphere) were compared. **Results:** PFV PET/CT reduced thoracic amplitude (80%), increased mean lesion SUV_{max} (29%) and SUV_{peak} (11%), decreased lung background SUV_{peak} (25%), improved lesion detectability, and increased SUV_{peak} lesion-to-background ratio (54%). On linear regressions, SUV_{max} and SUV_{peak} significantly improved (by 35% and 23%, respectively; $P \leq 0.02$). **Conclusion:** PFV-induced apnea reduces thoracic organ motion and increases lesion SUV, detectability, and delineation, thus potentially affecting patient management by improving diagnosis, prognostication, monitoring, and external-radiation therapy planning.

Key Words: PET/CT; High-Frequency Percussive Ventilation; HFPV; respiratory motion; Pulsatile-Flow Ventilation

J Nucl Med 2016; 57:416–419
DOI: 10.2967/jnumed.115.163386

PET/CT has become a major oncologic imaging modality for diagnosis, prognostication, therapy monitoring, and radiation therapy planning (*1*). Respiratory motion has significant negative effects on image quality, on the accuracy with which PET quantifies lesion activity, on fusion accuracy, and on delineation of lesion volume (*2*). Several advanced PET/CT respiration-gating techniques have been developed to palliate thoracic organ motion (*2*). All have intrinsic limitations, such as longer PET acquisitions, mixing of several tissue positions in a single bin, and difficulty with irregular breathing patterns. In addition, not only PET but also CT should be gated to avoid introducing supplementary attenuation correction and quantification errors (*2*). Today, these techniques are not universally applied and no consensus exists as to the best method to compensate for respiratory motion.

HFPV (high-frequency percussive ventilation; OxyCare GmbH) was first designed to promote airway clearance through a percussive flow of air. On the basis of this hygienic effect, HFPV was then developed in inpatient burn units, with percussive airflow favoring evacuation of airway debris secondary to inhalation injury (*3*). The physical principle is to deliver high-frequency ventilation (>400/min) in low ventilation cycles (10–30 cycles/min). Clinical experience demonstrated improved lung compliance, oxygenation, and ventilation compared with conventional ventilation in intensive care. These benefits extended the indication as a salvage modality for acute respiratory distress syndrome, with clinical evidence supported by smaller trials. Successive subtidal breathing with added high-frequency oscillations to both the inhalation phase and the exhalation phase facilitates oxygen diffusion and carbon dioxide removal. We refined this technique to obtain apnealike respiratory motion stabilization at full inspiration for medical imaging and radiation therapy (*4*). We achieved apnea lasting 8–16 min, allowing radiation therapy in nonintubated patients (*4*).

We aimed at establishing Pulsatile-Flow Ventilation (The BIRD Institute of Pulmonary Care, Villeneuve-Loubet, France) PET/CT (PFV) to suppress respiratory motion and quantify lesion detectability and quantification.

MATERIALS AND METHODS

Patient Population

Four patients (mean age ± SD, 65 ± 14 y) with a pulmonary tumoral lesion (mean size, 11 ± 7 mm; range, 5–18 mm) deemed treatable by radiation therapy were assessed in this research protocol, which was authorized by the State of Vaud Ethics Committee on Human Research. All patients signed an informed consent form. We had originally enrolled 5 patients (between November 2014 and April 2015), but 1 patient refused to undergo PFV PET/CT. The clinical characteristics of the 4 assessed patients are presented in Table 1.

^{18}F-FDG PET/CT Acquisition

Images were acquired on a time-of-flight PET/CT scanner (Discovery D690; GE Healthcare) with scatter and point-spread-function recovery corrections, 60 min after injection of ^{18}F-FDG (3.5 MBq/kg) and after the patients had fasted for at least 6 h (PET: 2 min/bed position, 47 slices, 256 × 256 matrix, ordered-subsets expectation

Received Jul. 5, 2015; revision accepted Nov. 16, 2015.
For correspondence or reprints contact: Jean Bourhis, Lausanne University Hospital, Bugnon 46, 1011 Lausanne, Switzerland.
E-mail: jean.bourhis@chuv.ch
*Contributed equally to this work.
Published online Dec. 3, 2015.

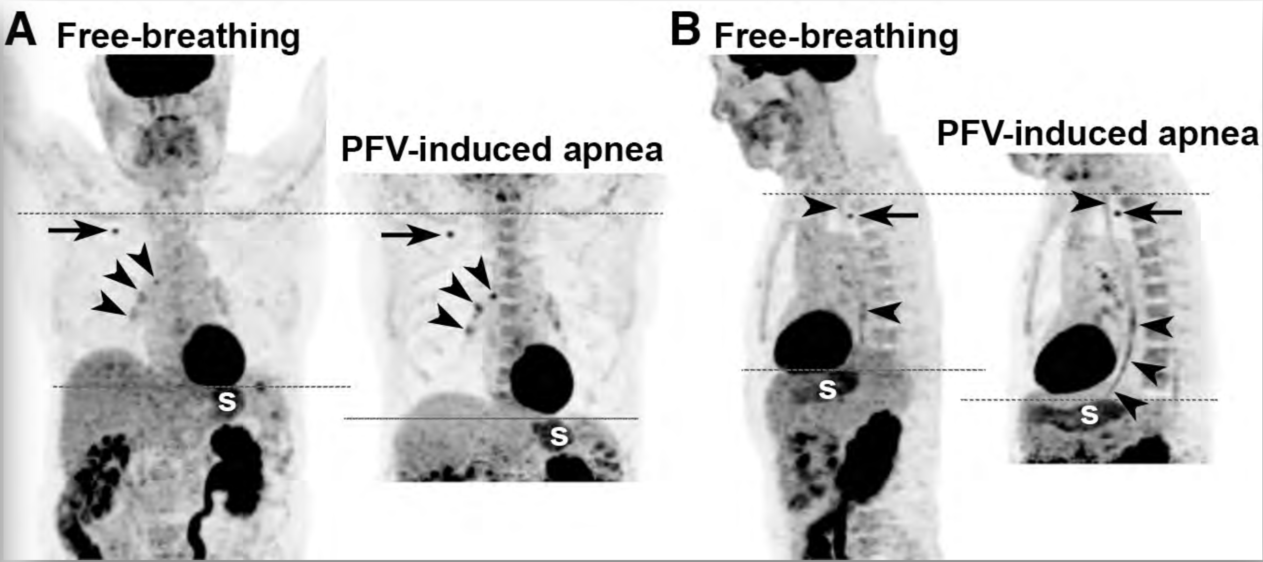

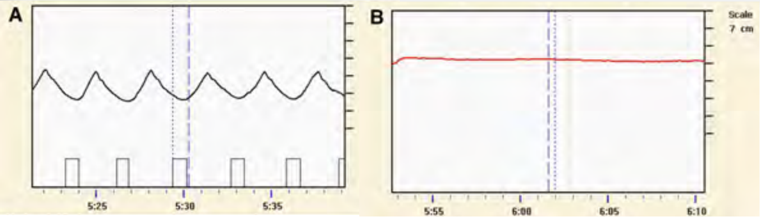

Prior et al, JNM 2016

Free-breathing vs. "Breath-hold" PET

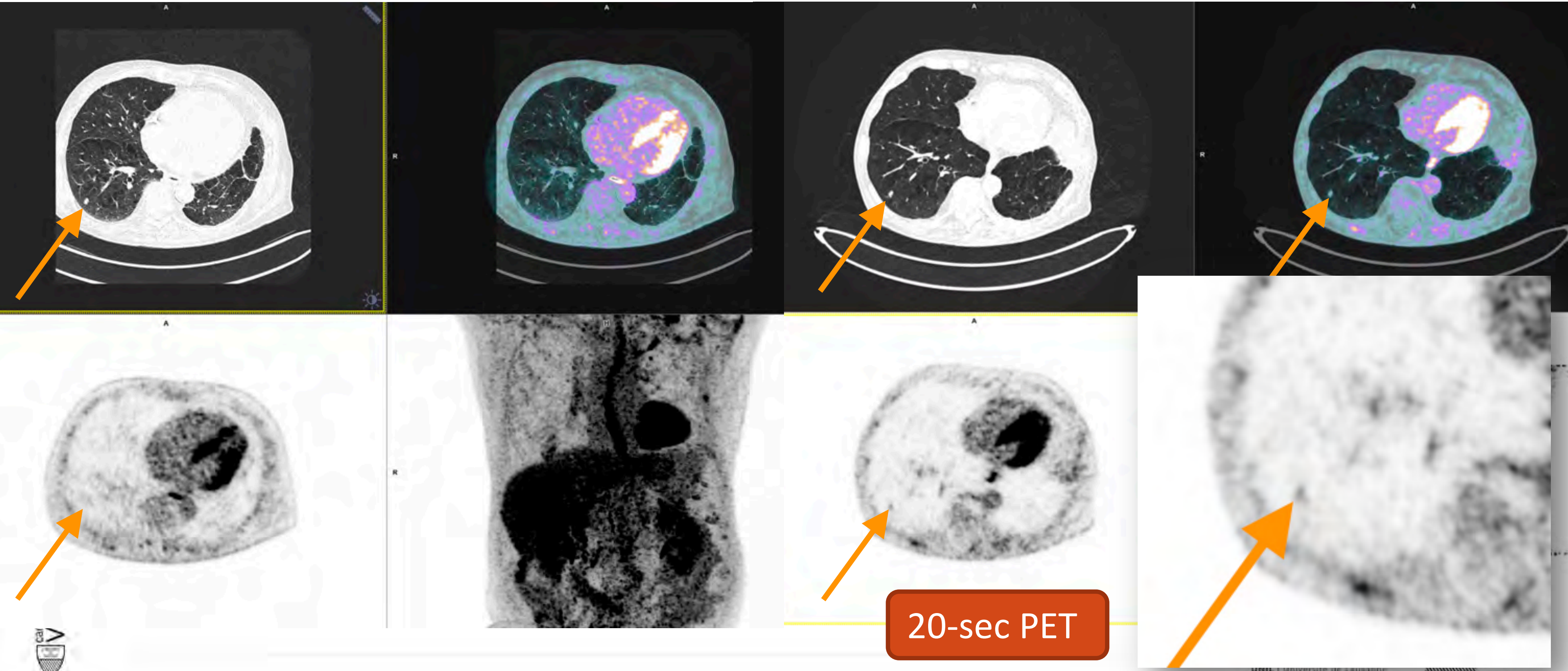

Free-breathing vs. “Breath-hold” PET

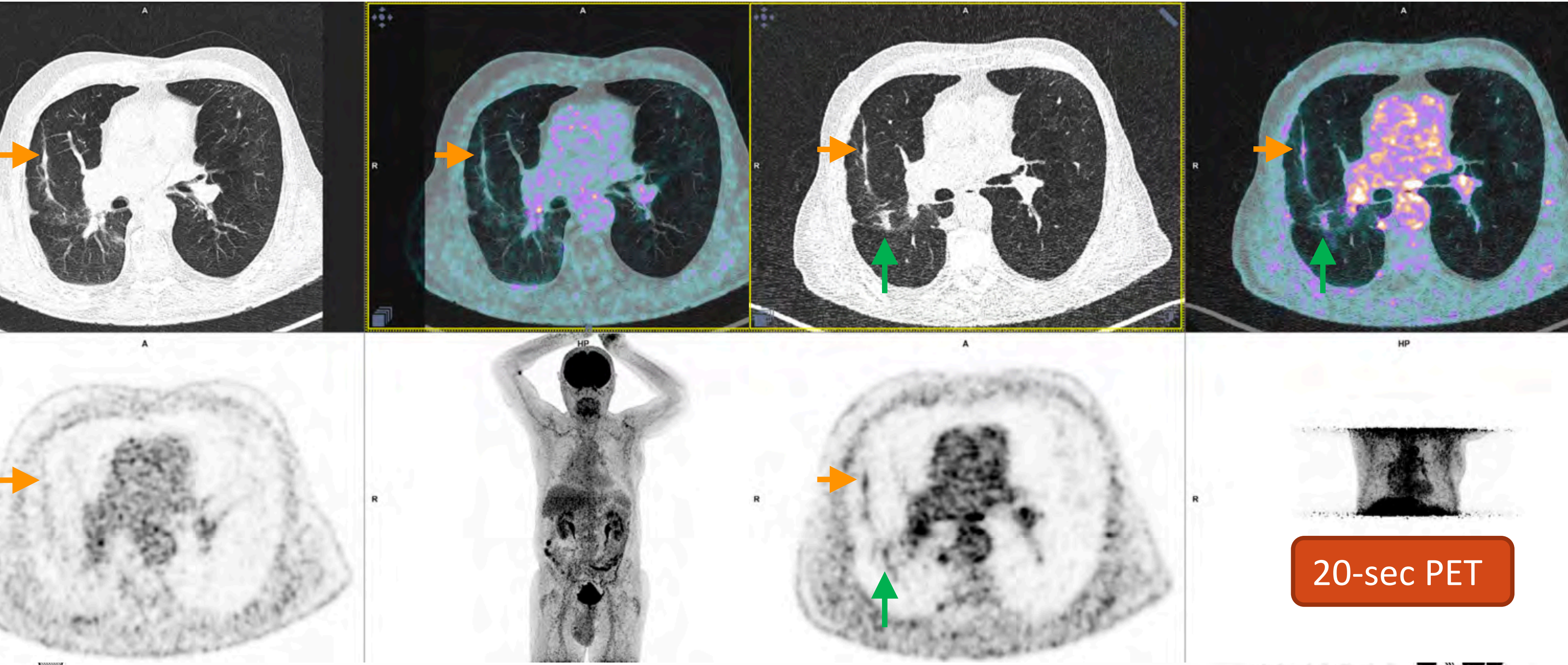

Importance for lung cancer screening?

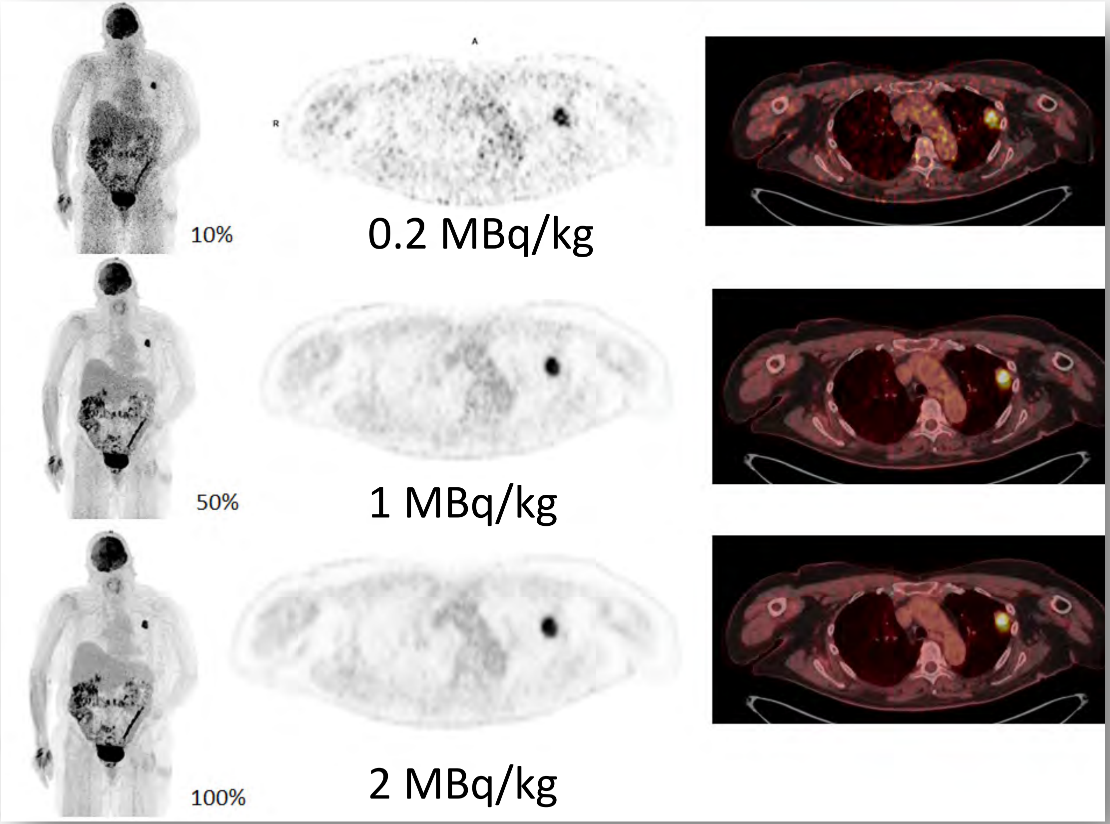

N=6 patients with lung nodule (15±8 mm)

100%, 50% and 10% of activity decimated reconstructions, 90-s/bed position

→SUV_{mean} decreased by 10% in 0.2 MBq/kg with stable signal-to-background ratio

Prior et al, Virtual SNMMI 2020

Ga-68-PSMA-11 PET/CT Staging Primary PCa

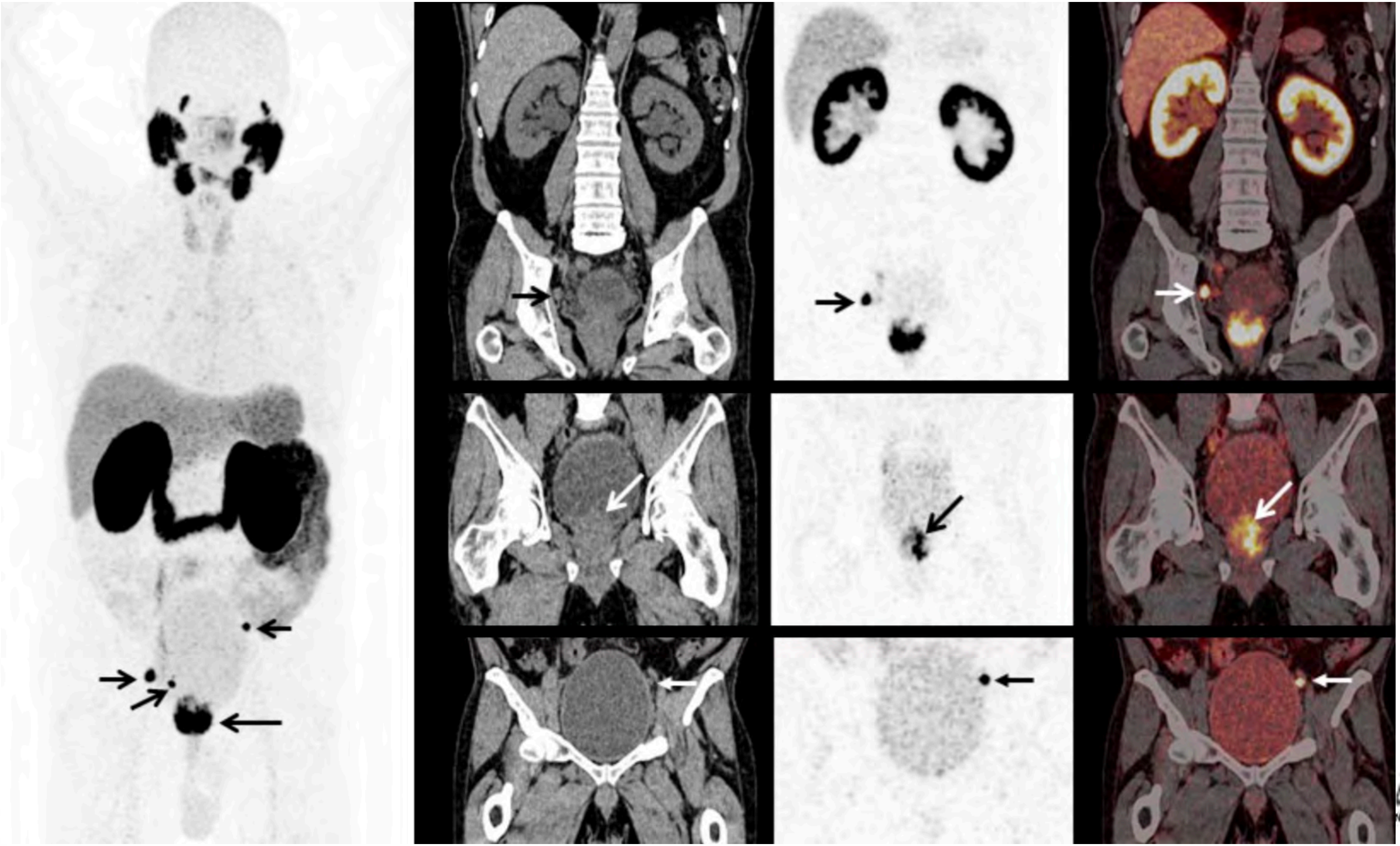

62-y Men with primary PCa

Ga-68-PSMA PET/CT Staging Primary PCa

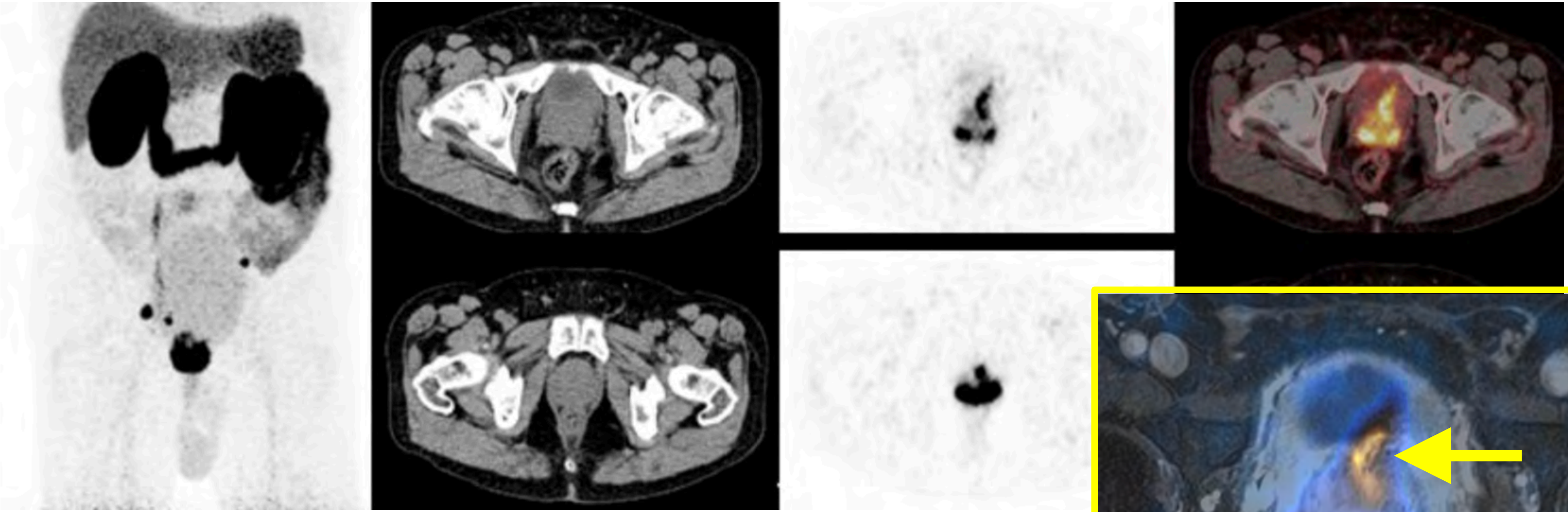

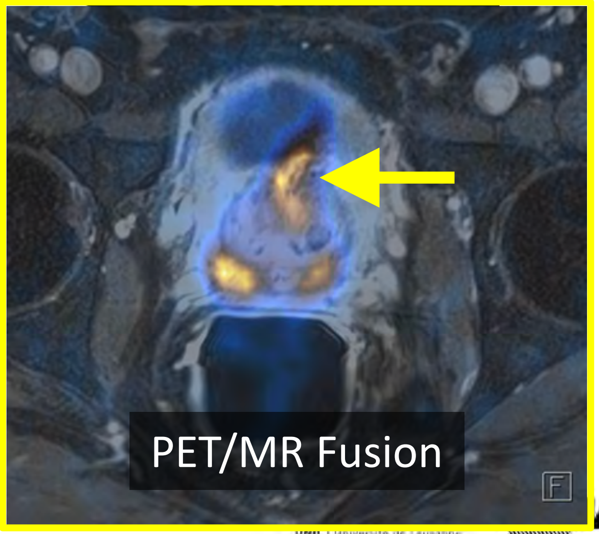

Ultrafast PET (<5-min)

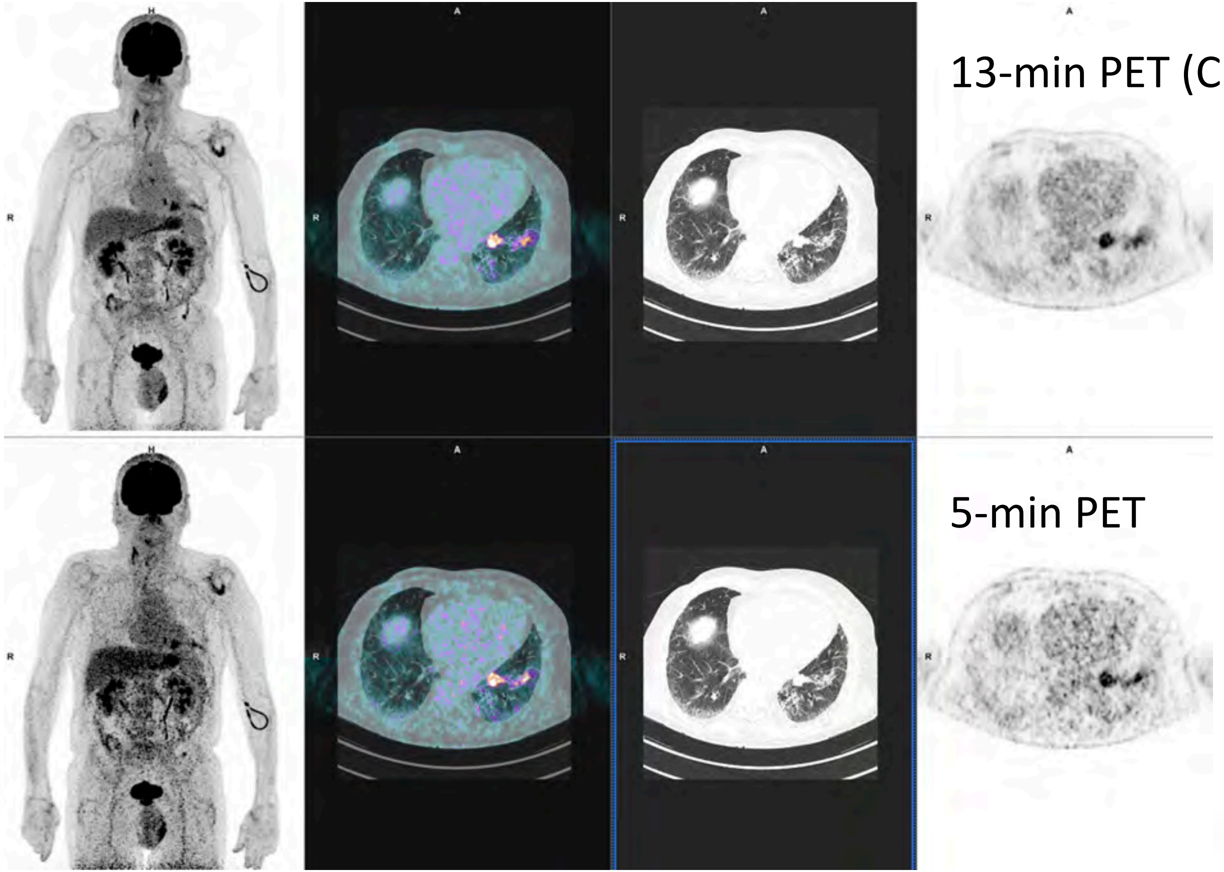

13-min PET (CBM, 1.5-min/bed equivalent)

5-min PET

→ Identical SUV measurements

Ultrafast whole-body PET (<5-min)

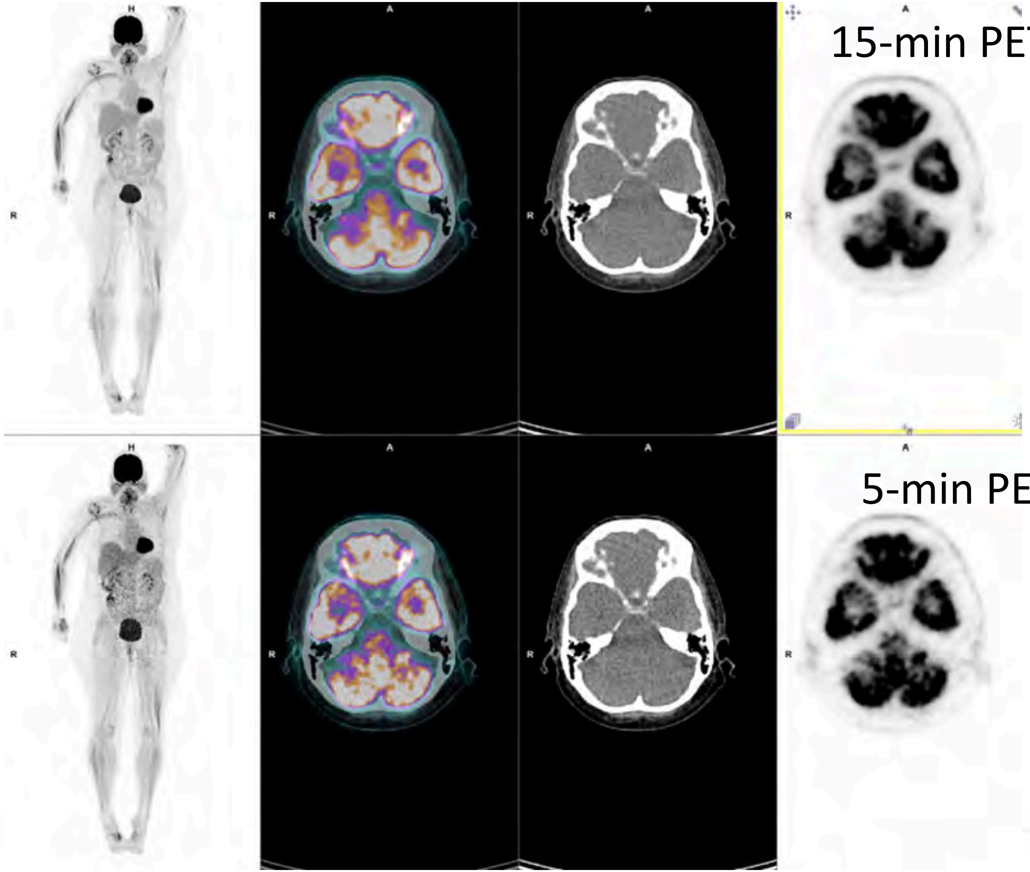

→ *Identical SUV measurements*

Less dose exposition

3.5 MBq / kg

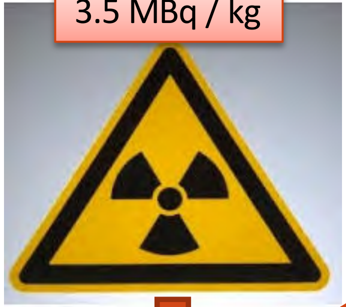

Patient Dose

Technologists and Staff dose

Public (returning @work or @home)

2 MBq / kg

–42% Reduction Activity & Dose

Automated injectors:
– More patient with same vial
– Less manipulation of activity

Brain PET

cPET

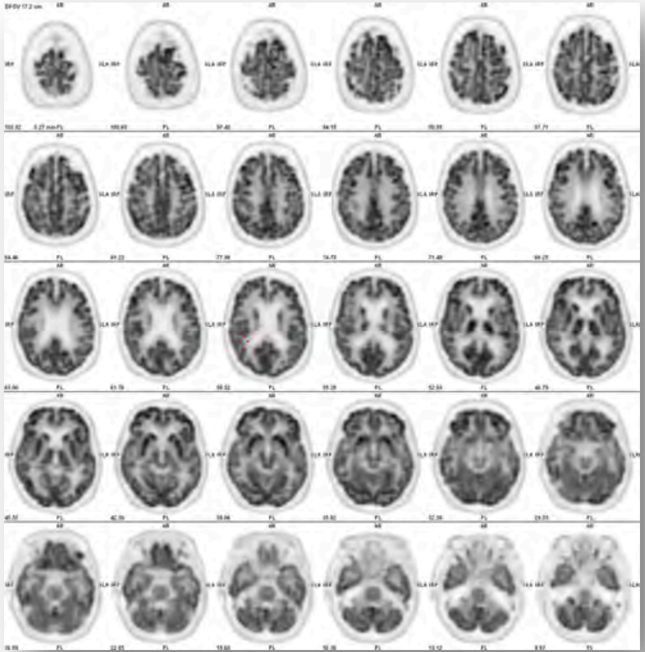

dPET

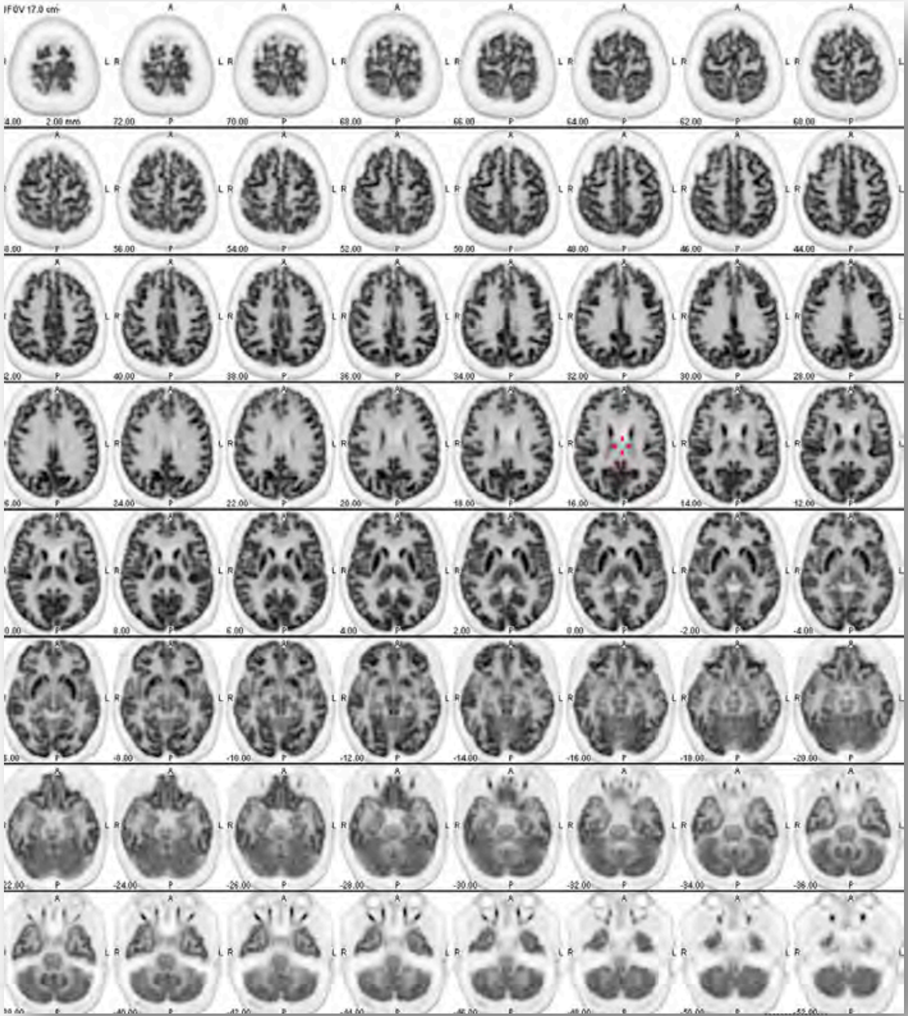

Rubidium-82 Cardiac-PET

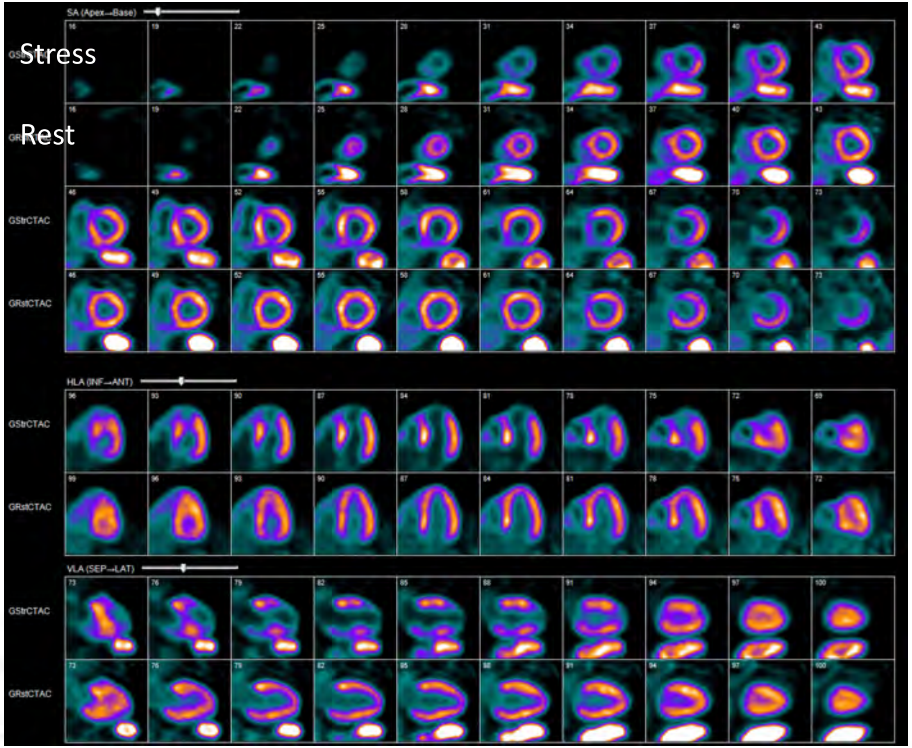

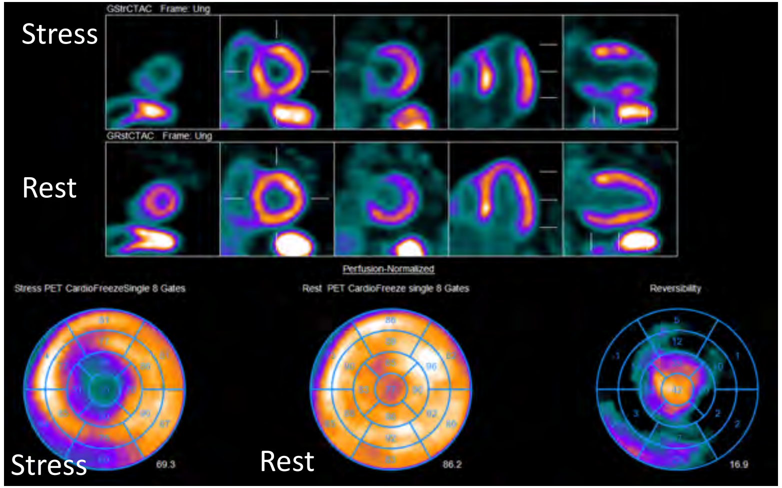

5 MBq/kg Rb-82 (86 kg) 430 MBq
6-Min Stress + Rest acquisitions

Reducing Rb-82 activity in cardiac PET/CT

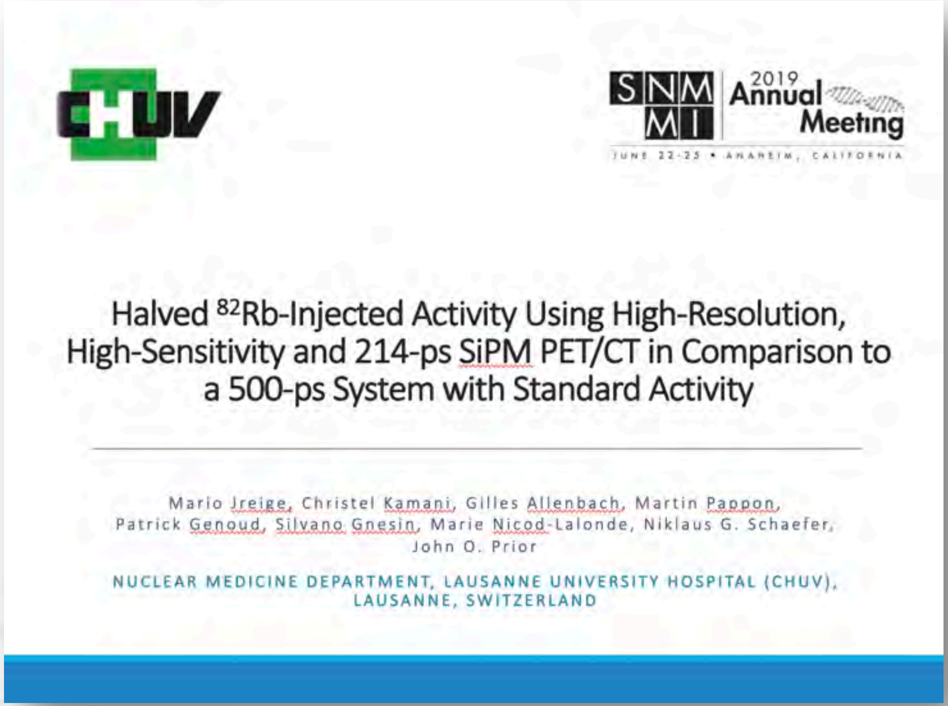

- 10MBq/kg with 500-ps cPET
- 5 MBq/kg with 214-ps dPET
- N=12 individuals with normal MBF in each group

Comparison 10 MBq/kg vs. 5 MBq/kg

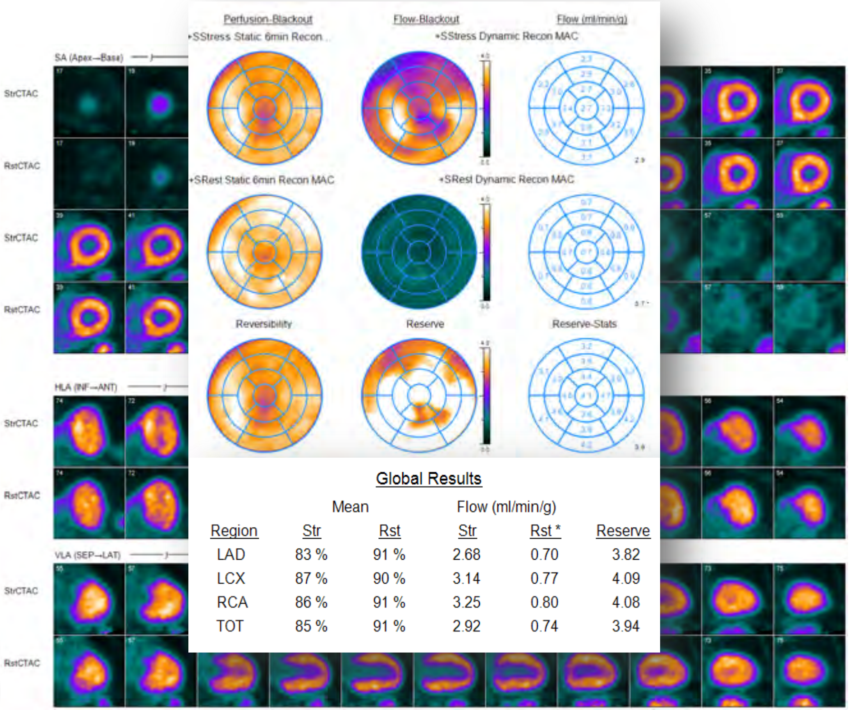

Region	Mean Str	Mean Rst	Flow (ml/min/g) Str	Flow (ml/min/g) Rst *	Reserve
LAD	83 %	91 %	2.68	0.70	3.82
LCX	87 %	90 %	3.14	0.77	4.09
RCA	86 %	91 %	3.25	0.80	4.08
TOT	85 %	91 %	2.92	0.74	3.94

500-ps TOF cPET

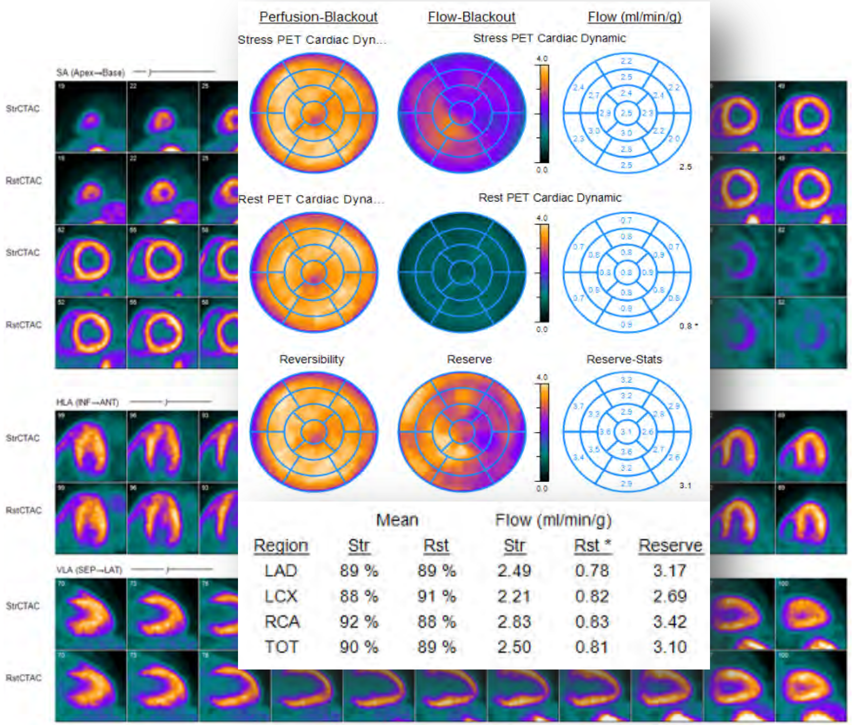

Region	Mean Str	Mean Rst	Flow (ml/min/g) Str	Flow (ml/min/g) Rst *	Reserve
LAD	89 %	89 %	2.49	0.78	3.17
LCX	88 %	91 %	2.21	0.82	2.69
RCA	92 %	88 %	2.83	0.83	3.42
TOT	90 %	89 %	2.50	0.81	3.10

214-ps TOF dPET

Results

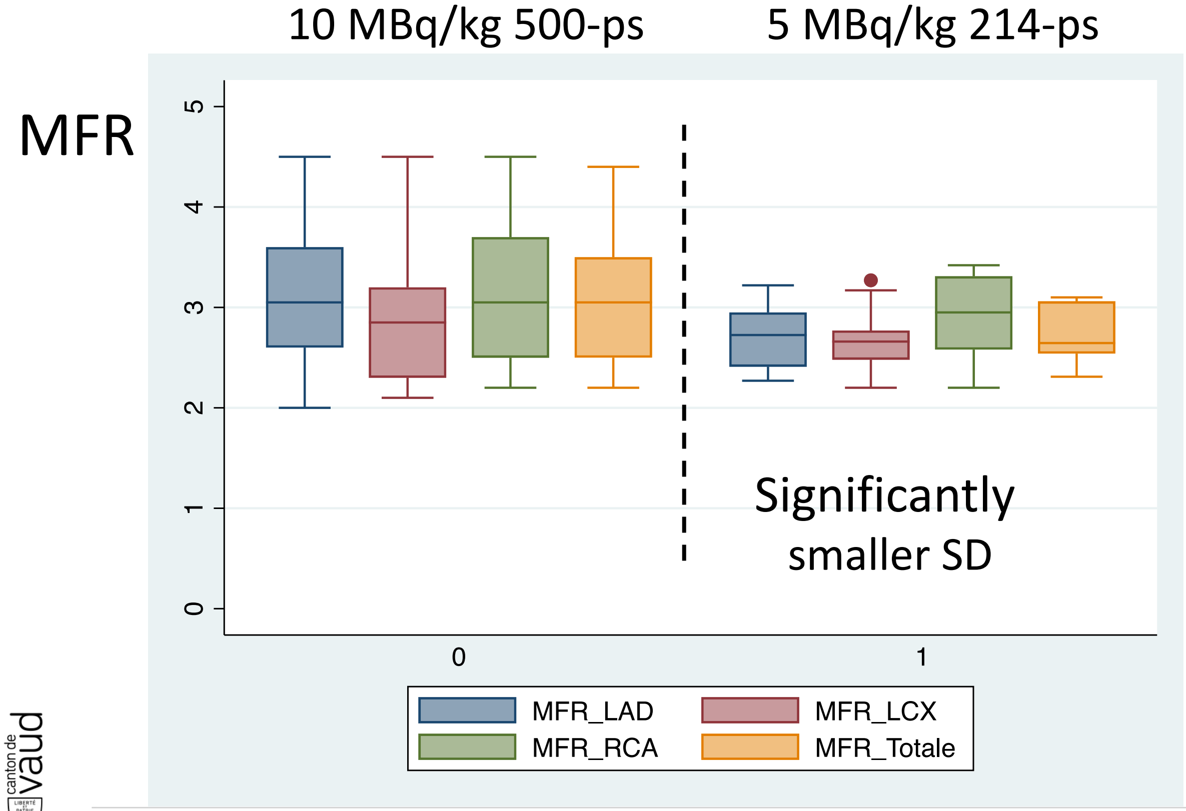

No. 101
01:00 PM
Halved82Rb-Injected Activity Using High-Resolution, High-Sensitivity and 214-ps SiPM - PET/CT in Comparison to a 500-ps System with Standard Activity.
Mario Jreige, Lausanne University Hospital

Y-90 TOF PET after SIRT

$32 \cdot 10^{-6}$ pair production

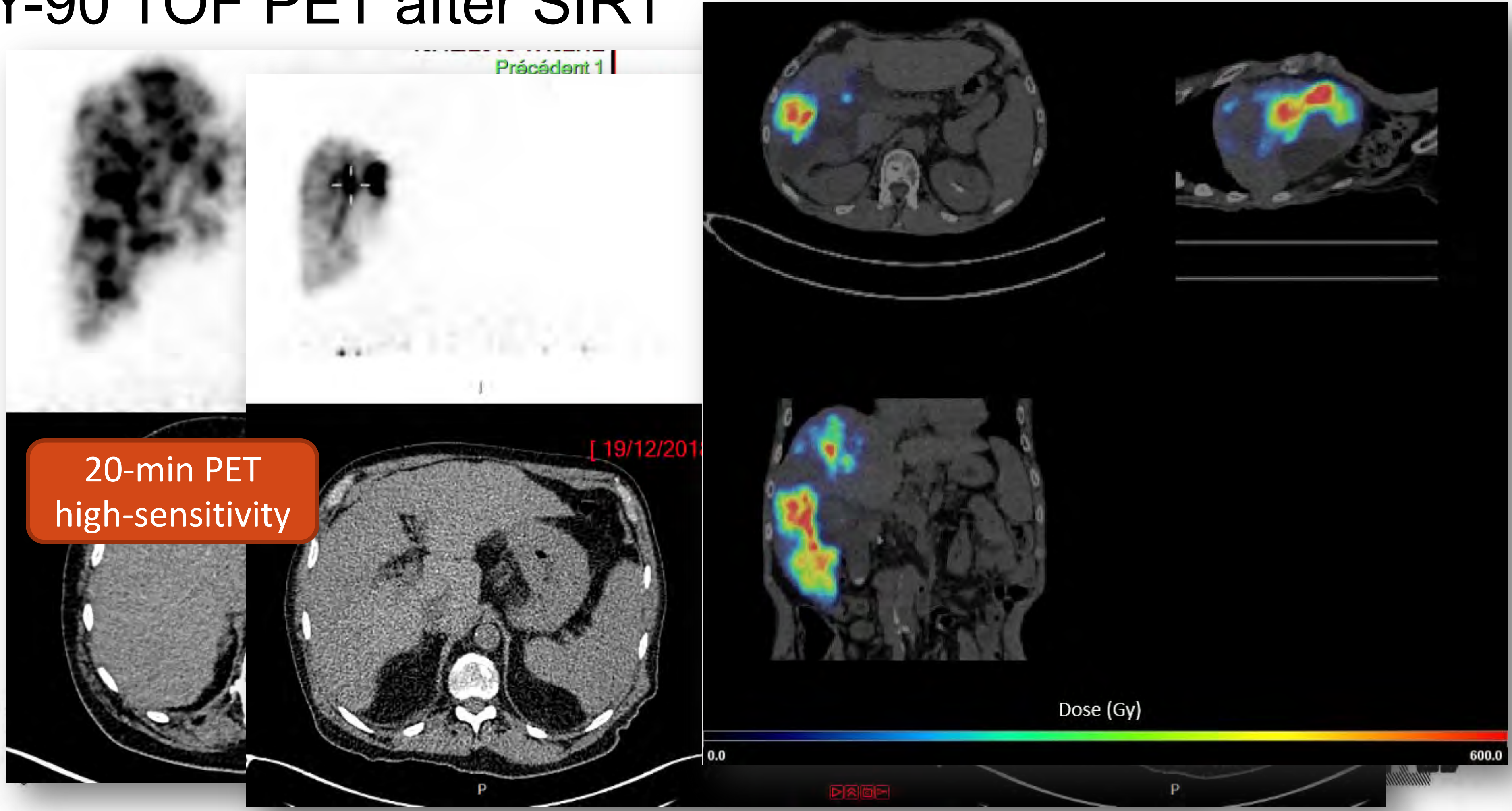

Total-Body PET Axial Length vs. Cost

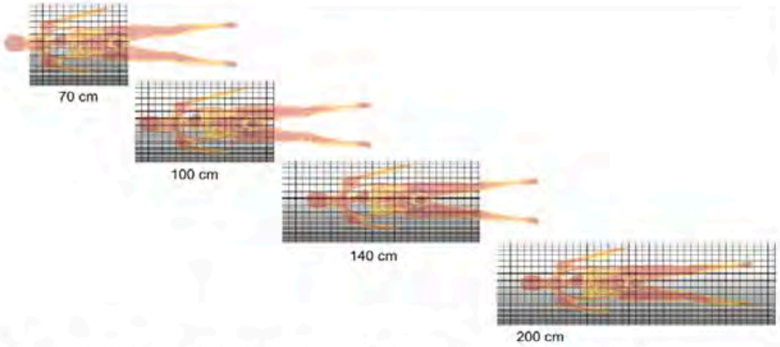

Fig. 8 Total body PET systems with an axial length of 70 cm, 100 cm, 140 cm and 200 cm

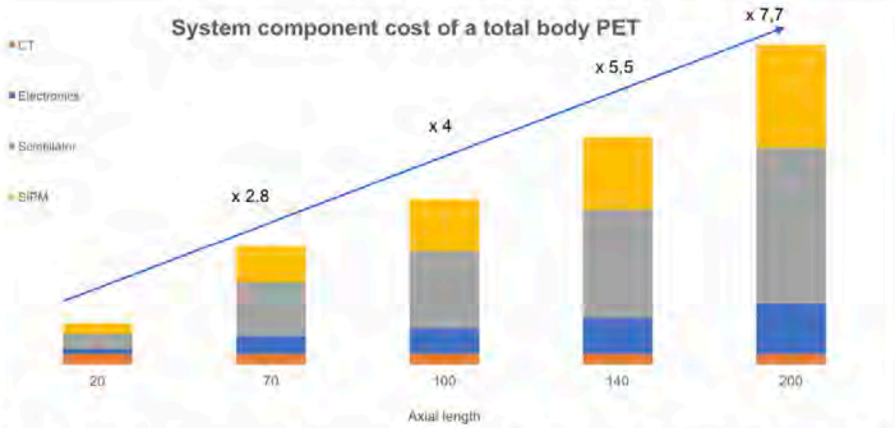

Fig. 9 Increase in component costs for a 70-cm, 100-cm, 140-cm and 200-cm system versus a system with 20 cm axial length; the *y*-axis is the system cost in relative units

Base Price PET 20-cm → 2 MCHF

Vandenbergh EJNMMI Physics 2020;7:35

Total-body PET (Explorer, 2m)

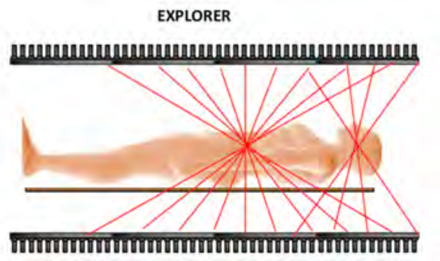

2 m de long
560’000 cristaux
PET en 30-40 seconds ou 1/40 l’activité habituelle

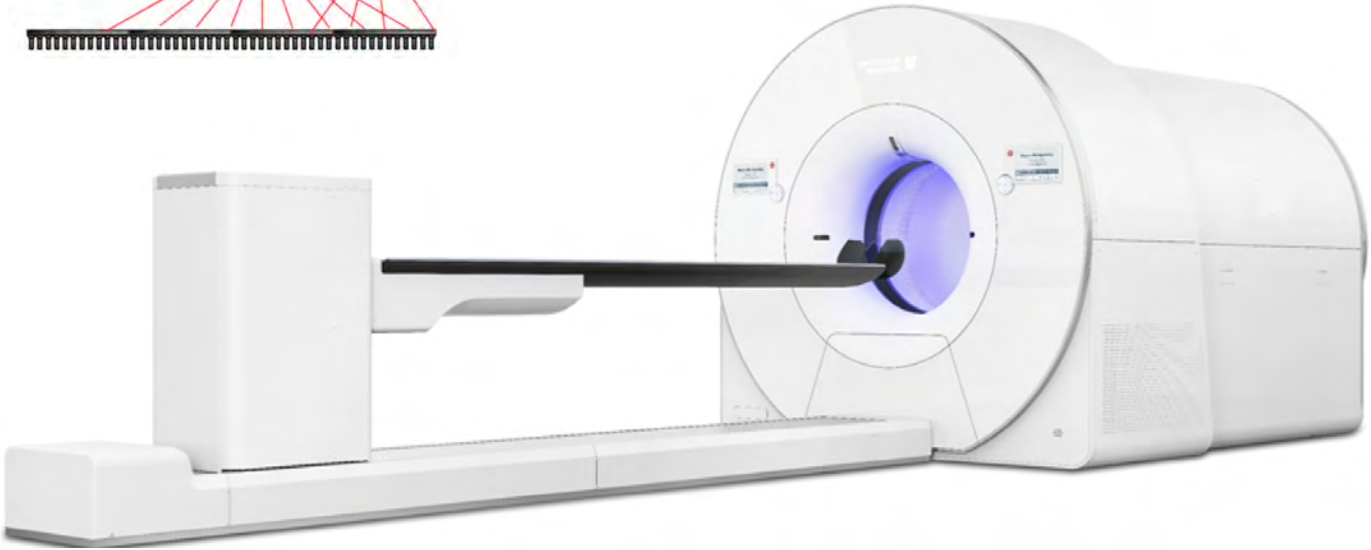

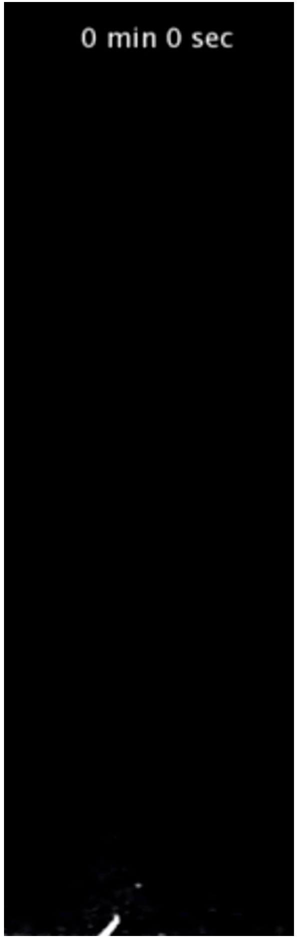

JNM 2019;60:299–303

https://youtu.be/JaszDkmgfMY

Total-body PET (Explorer, 2m)

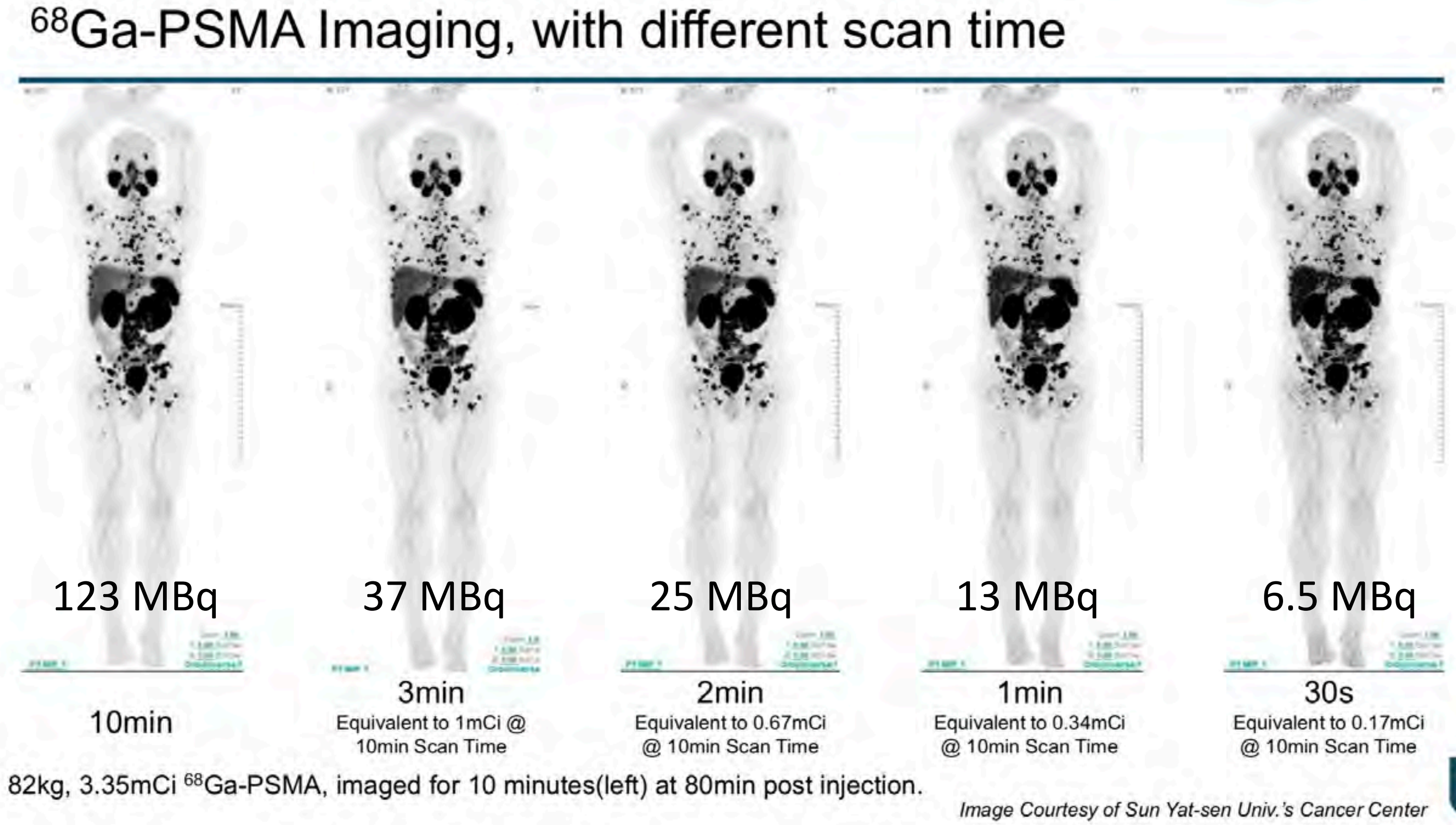

High sensitivity (total body) imaging

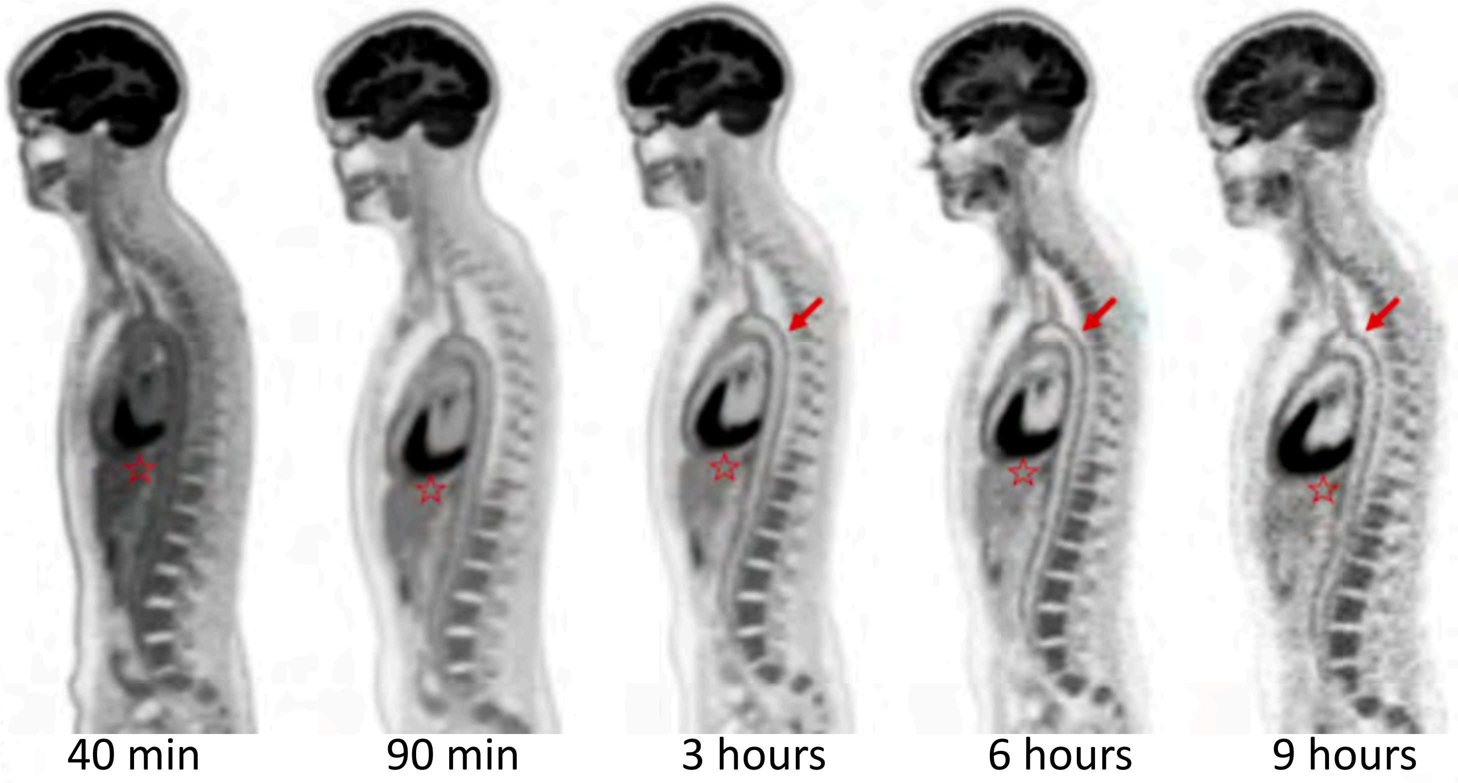

Comparable image quality at 9 hours as today's clinical system at 1 hour

L. Nardo et al, PET Clin 2020:271

Total-Body PET/CT Captures Full Picture of Systemic Inflammatory Arthritis

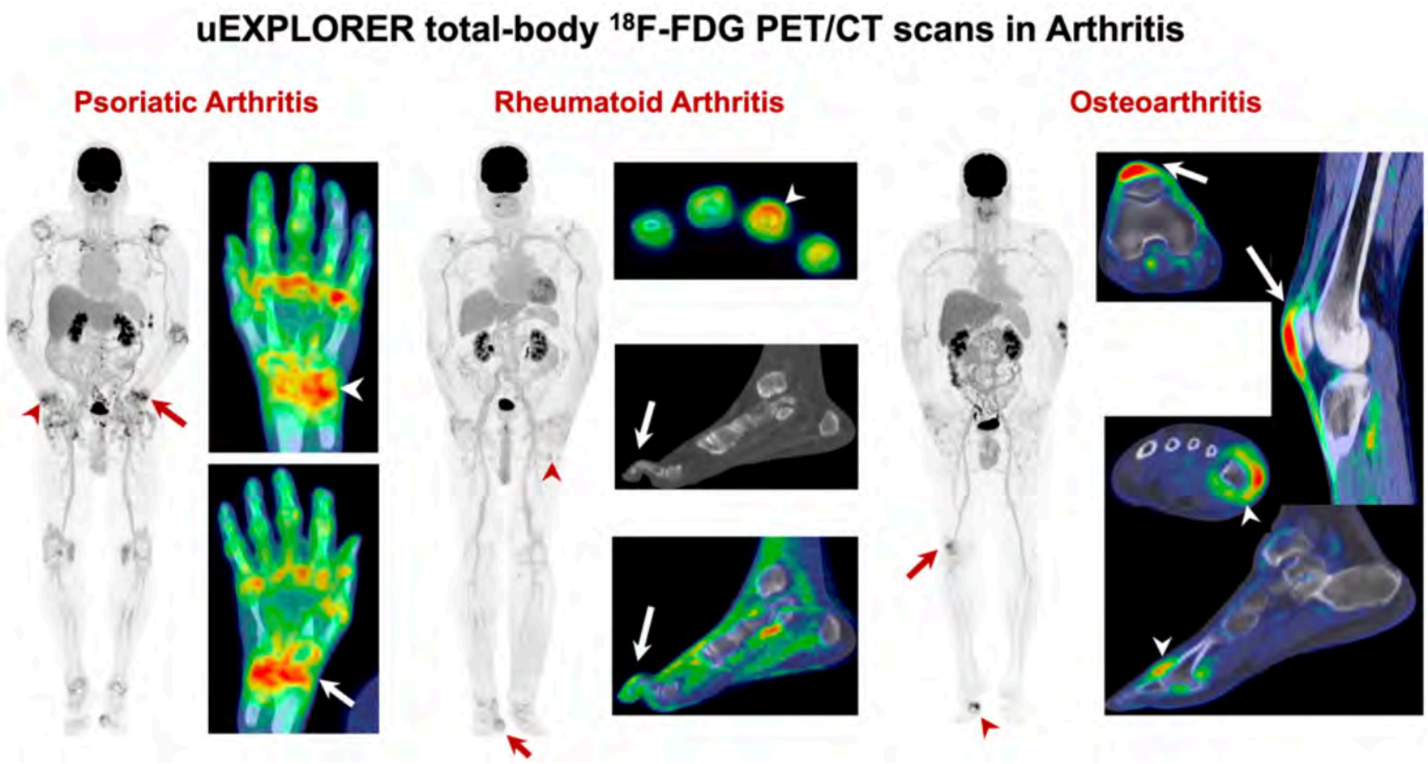

Low radiation dose:
20-min scan
75 MBq F-18-FDG
→ 1.4 mSv

Abdelhafez et al., University of California Davis, Virtual SNMMI 2020

Total-body PET (Explorer, 2m)

Benefits:

- Better
- Faster
- Later after injection
- Lower dose
- Total-body dynamic

- **Major increase in dynamic range**

  can image for 5 more half lives

- **^{11}C**

  > 3 hours

- **^{18}F**

  > 16 hours

- **^{89}Zr**

  > 30 days

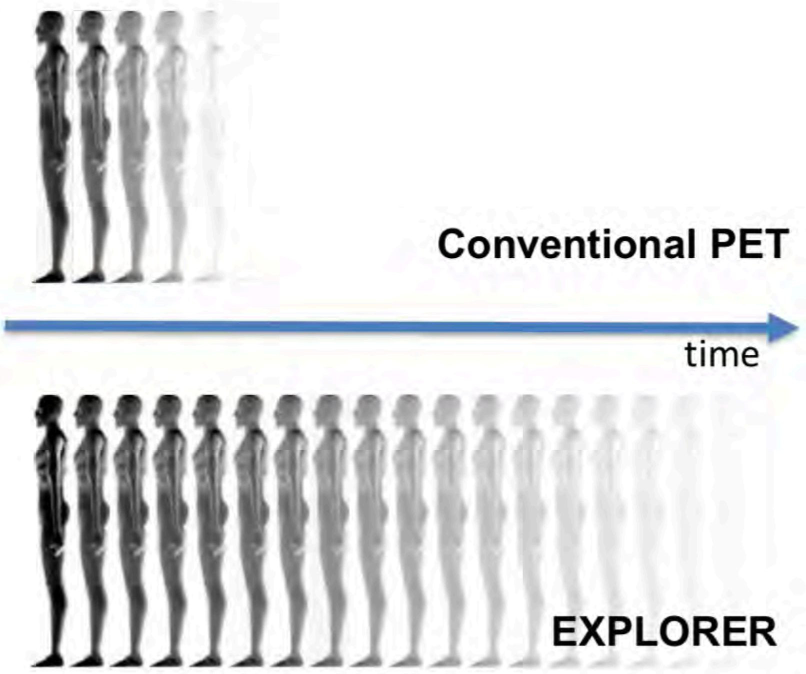

Long axial FOV PET

1.06-meter

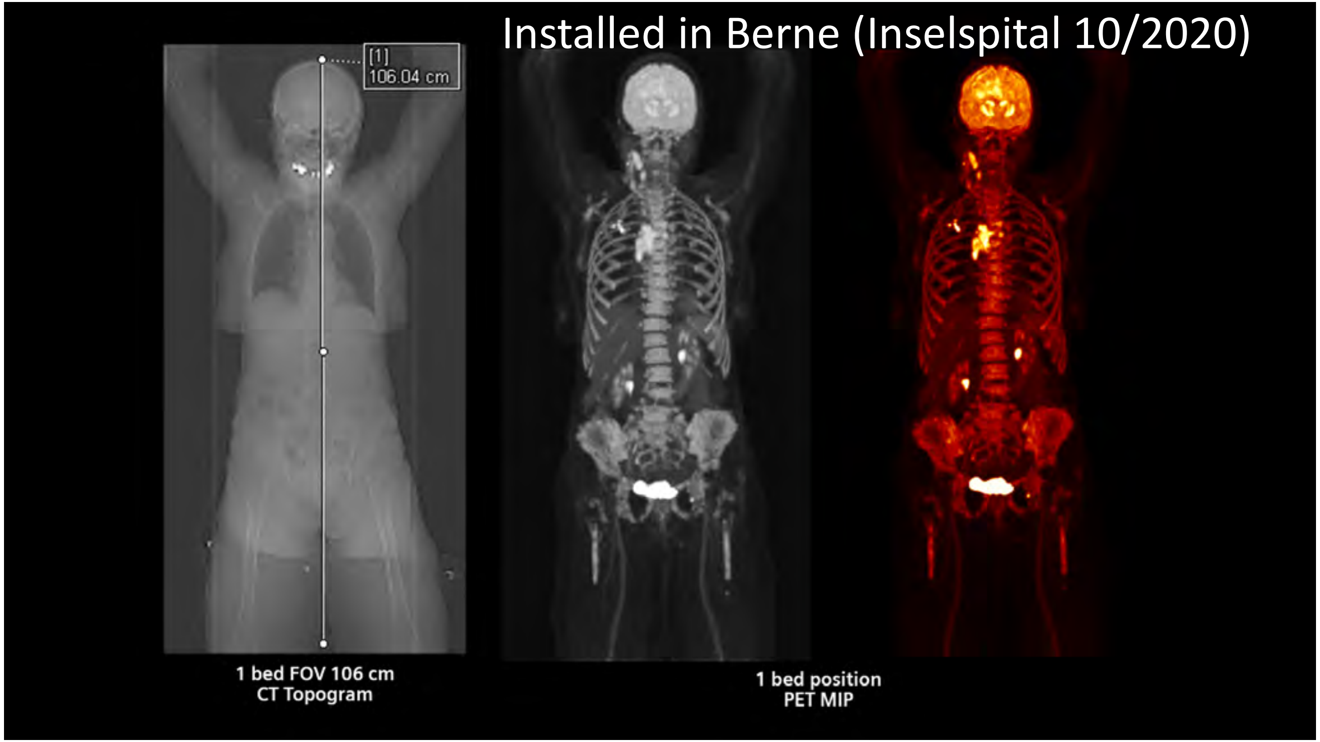

https://www.siemens-healthineers.com/molecular-imaging/pet-ct/biograph-vision-quadra

10-min
PET

→190 MBq

4-min
PET

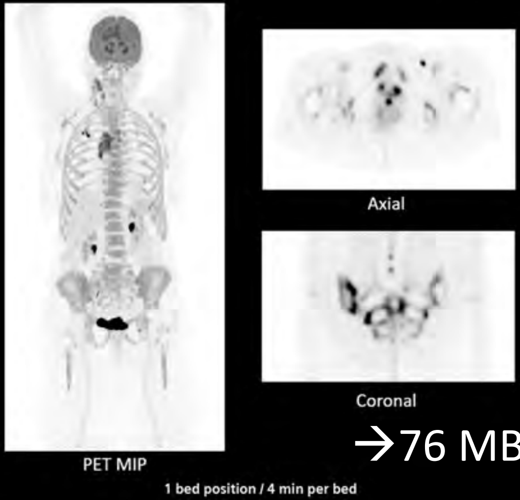

→76 MBq

1-min
PET

→19 MBq

15-s
PET

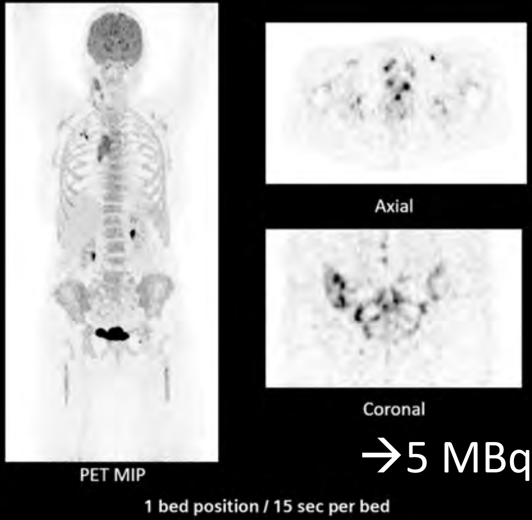

→5 MBq

https://www.siemens-healthineers.com/molecular-imaging/pet-ct/biograph-vision-quadra

PET: 3 major improvements last 3 decades

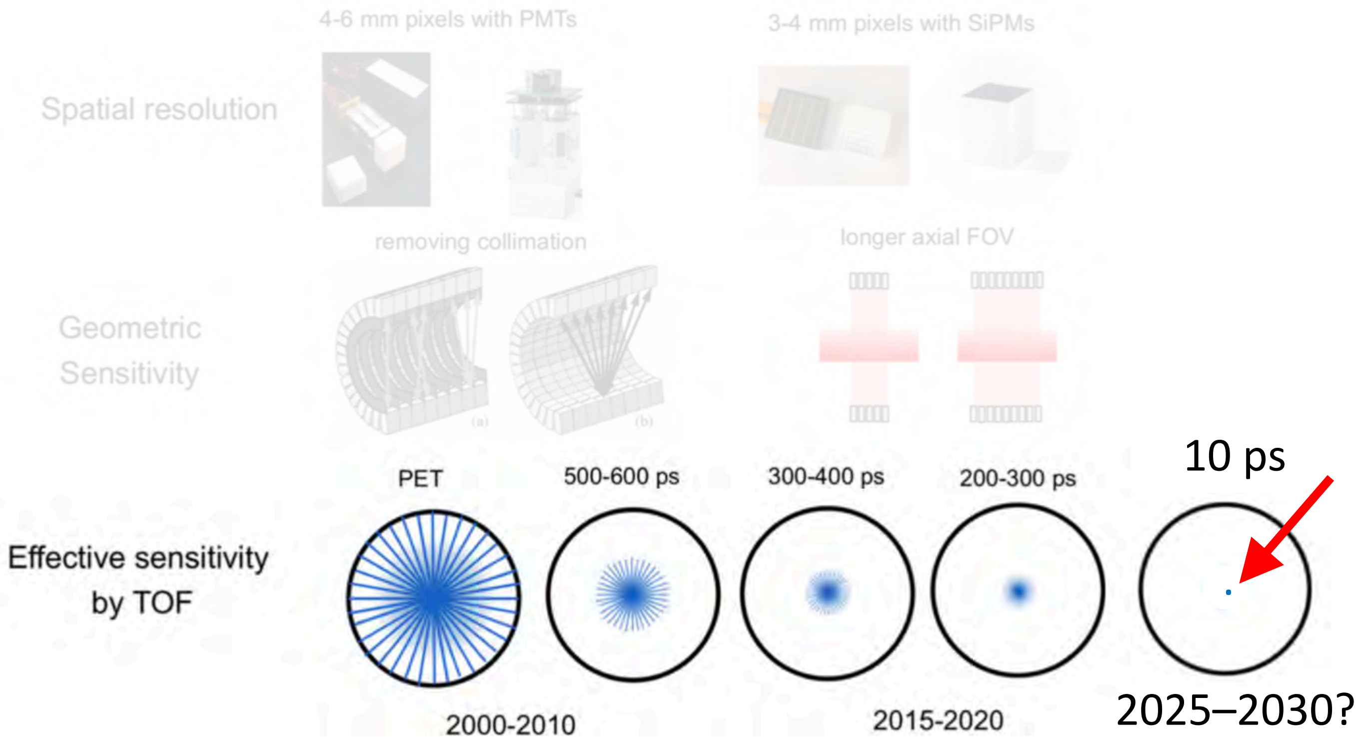

Vandenbergh EJNMMI Physics 2020;7:35

10-ps TOF PET: Advantages

Next technology?

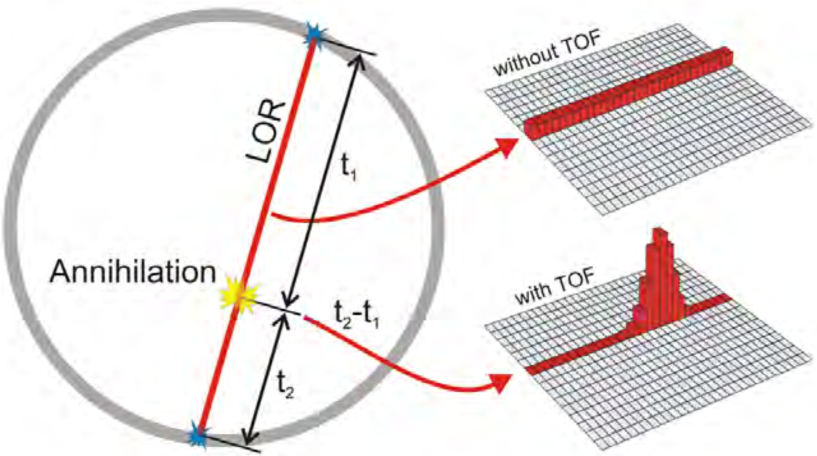

P. Lecoq, C. Morel, J. Prior, 2018

- 1.5-mm resolution along LOR
- Tomography-less real-time reconstructions ("Anger-camera"-like)
- Total-body with sparse detectors
- Increase PET sensitivity (>16)
- Reduction in activity per dose, reduced price
- Better quantification @low count → ultra low-dose screening (oncology, psychiatric & infectious diseases)

Clinical improvements

Better resolution (tumor microenvironment)

Better sensitivity

- Less activity
- Image longer (C-11 4h, F-18 20h, Zr-89 30d)
- Image faster (respiratory/cardiac/GI movements)
- High temporal resolution
- 200-fold reduction (0.03 mSv = 2.5d natural irradiation)
- Image more often

Novel clinical applications (1)

Precise quantification of low-activity metabolism, such as apoptosis (programmed cell death) in myocardial infarct, chronic heart failure, stroke or neurodegeneration (Alzheimer or Parkinson's disease)

→may help to develop new drugs or better follow and treat disease activity

Novel clinical applications (2)

Lung cancer screening (with CT: now 96% false positive rate) → better with ultra-low-dose PET

Non-fatal disease: tuberculosis (India, China, South Africa, $10 \cdot 10^6$ new cases/$1.8 \cdot 10^6$ death in 2015), HIV, also

(schizophrenia, r

disorders)

SARS-CoV-2…

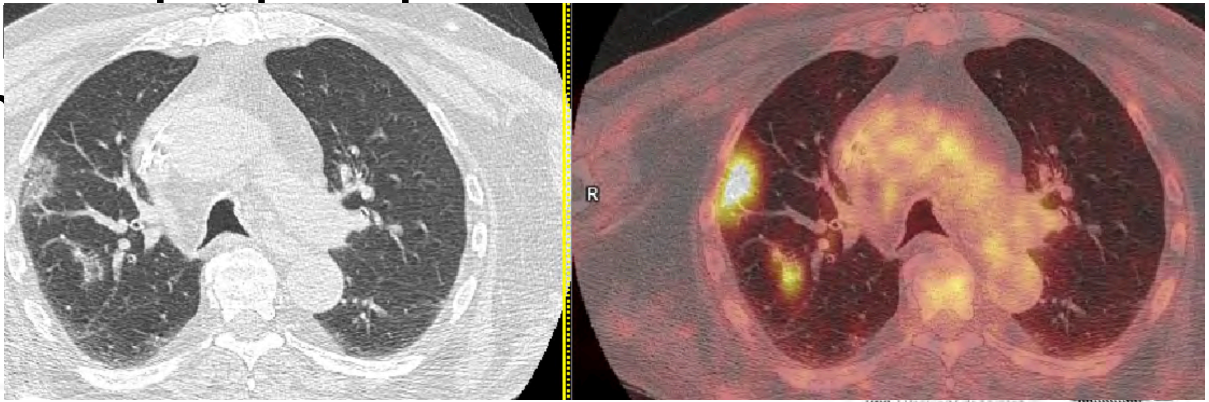

Novel clinical applications (3)

Radiation dose equivalent to a few days–weeks of natural radioactivity

Advantages for pediatric NM, but also for fetal growth and placental pathology (obstructive uropathy, brain development, hypoxic insult, abnormal fetal motor behavior and epilepsy) → benefit to percutaneous or fetal surgery, which has entered the clinical arena

10-ps TOF-PET improvement simulation

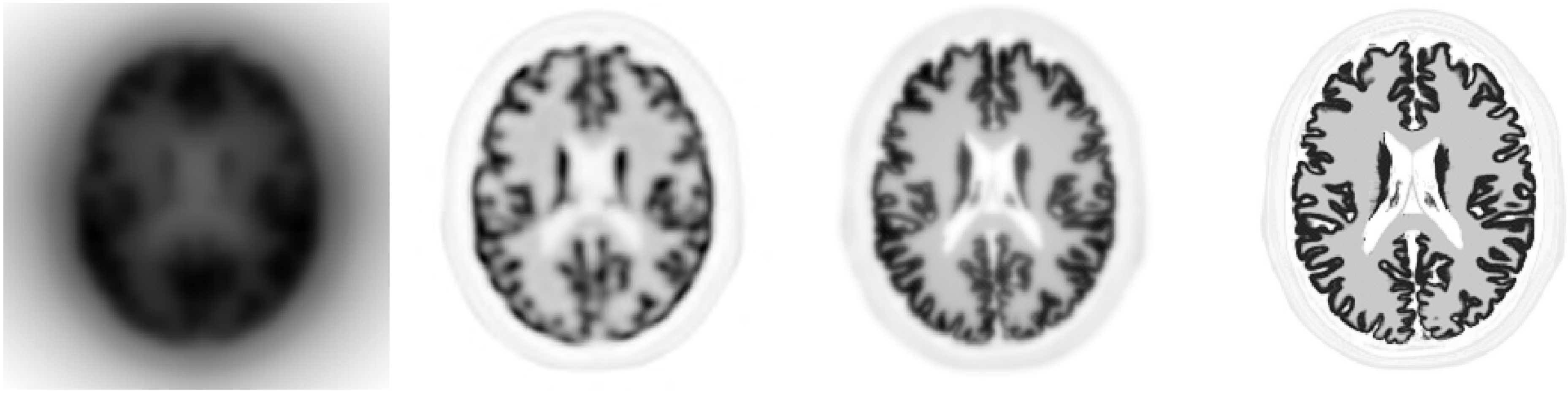

Non-TOF FBP	Non-TOF OSEM	10ps TOF FBP	10ps TOF OSEM

Johan Nuyts, UZ Leuven, 2018

Therefore…

Creation of the 10-ps TOF PET Challenge

http://the10ps-challenge.org

The 10ps challenge: a step toward reconstructionless TOF-PET

The 10ps challenge:

- a spur on the development of fast timing
- an opportunity to get together
- an incentive to raise funding
- a way to shed light on nuclear instrumentation for medical imaging

One unique challenge launched for 5 to 10 years and operated by an international organisation with rules issued by the community based on the measurement of CTR combined to sensitivity

Several milestones and prices:

- 3 years after the launch of the challenge: 1M€ expected for the Flash Gordon prices for the realisation of 3 important milestones
- until the end of the challenge: 1M€ expected for the Leonard McCoy price for the first team meeting successfully

http://the10ps-challenge.org

Endorsement

EANM

EUROPEAN INSTITUTE FOR BIOMEDICAL IMAGING RESEARCH

WMIS World Molecular Imaging Society Discover. Visualize. Learn. Cure

IEEE NPSS NMISC

PETsys Electronics

Worldwide:
42 PET Scientists
and Physicians

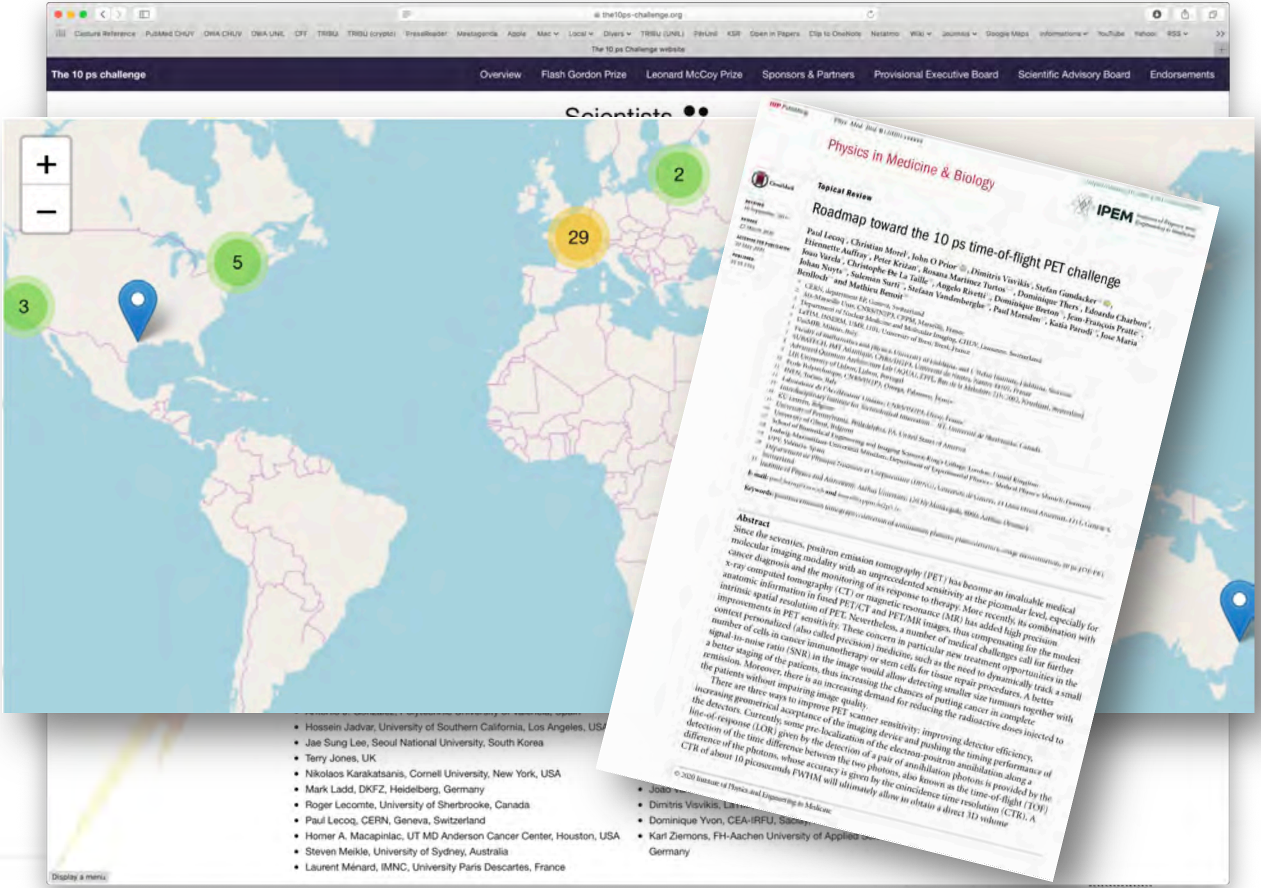

canton de vaud

As of January 2021

Part 2

Hybrid whole-body CZT gamma-camera

Hybrid whole-body CZT gamma-camera

(NM/CT 670 CZT)
NM/CT 870 CZT

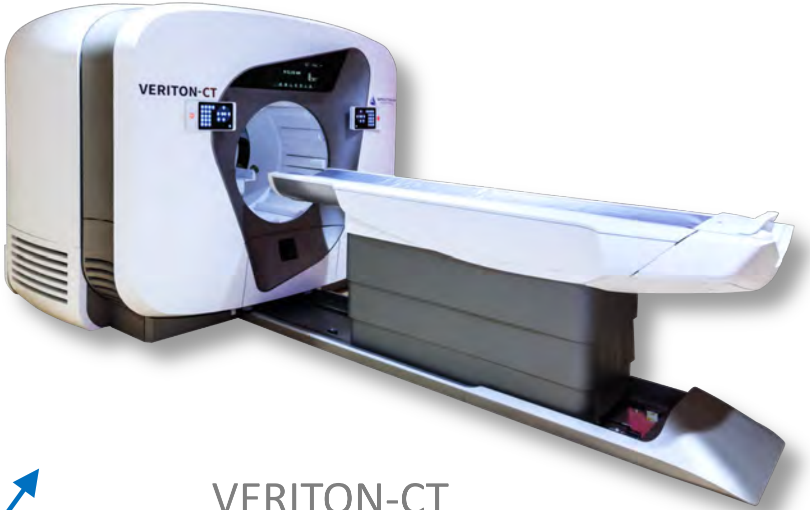

VERITON-CT

Different collimation systems

CZT detectors for nuclear imaging

1. **Direct** detection enabling **high detection efficiency**
2. **Small pixelated** detectors (2.46 mm, compact design)
3. **High energy resolution** (2 x higher than NaI(Tl))
4. **Currently a maximal energy** in the range ~200 keV for the detected photons

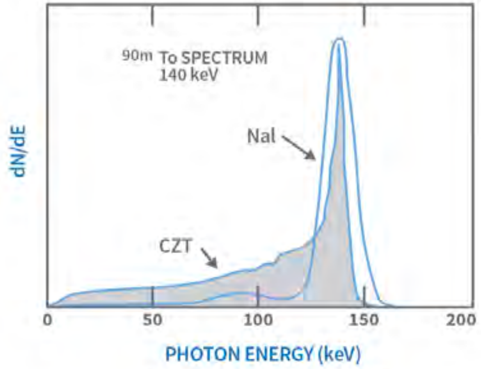

Barone-Rochette et al. JNC 2015

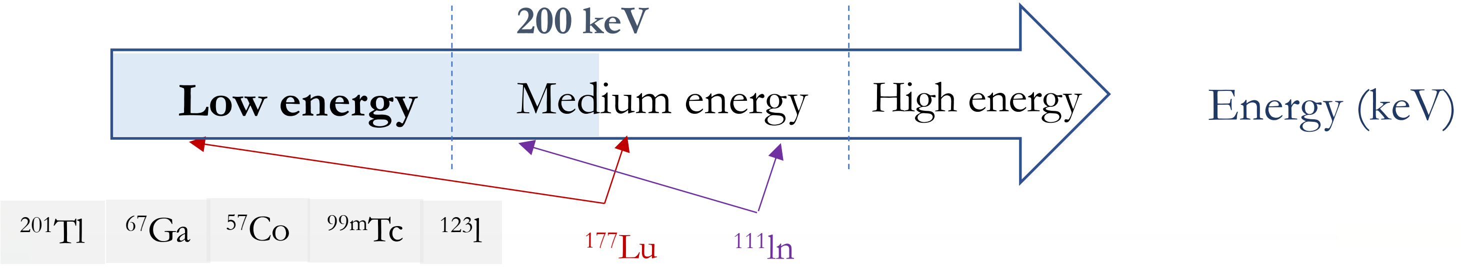

360° CZT VERITON™ system

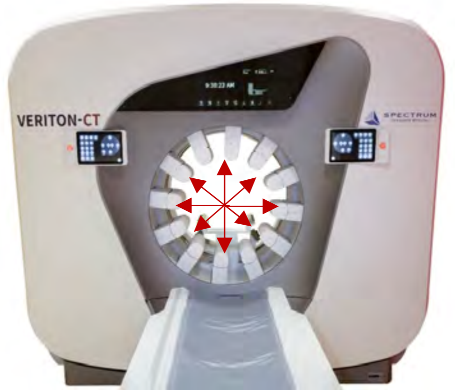

12 detectors

8 CZT modules per detector

Swiveling detectors in **close proximity** to the patient

Direct photon conversion

Full 360° FOV Scan	Focused 360°FOV Scan
Projections acquired from the entire FOV	80 to 100% of the projections acquired directly from a ROI

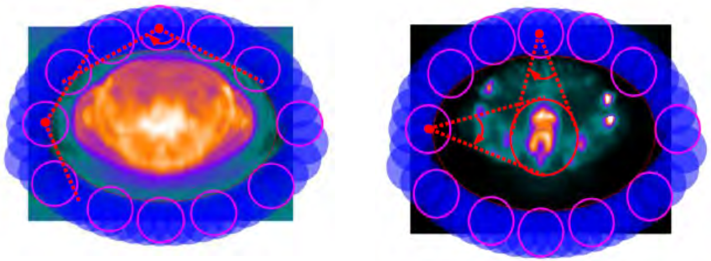

Myocardial perfusion SPECT

Decreased Activity & Time
Cardiac dynamic SPECT possibility (software exists)

Patient 01
Sex F
160 cm / 52 kg

Stress:
103 MBq – 10 min

Rest:
290 MBq – 5 min

Anterior infarction

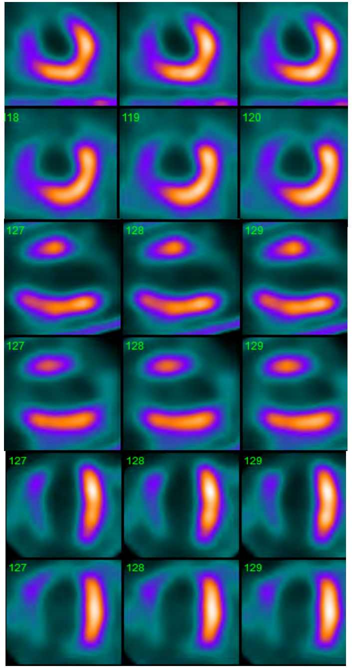

Stress SA
Rest SA
Stress VLA
Rest VLA
Stress HLA
Rest HLA

Patient 02
Sex M
173 cm / 85 kg

Stress:
150 MBq – 10 min

Rest:
461 MBq – 5 min

Apical ischemia

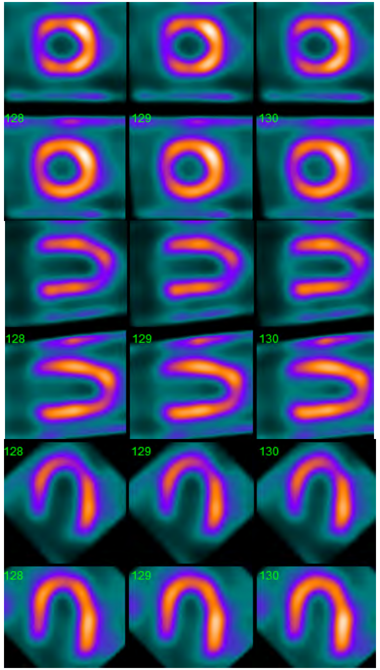

Stress SA
Rest SA
Stress VLA
Rest VLA
Stress HLA
Rest HLA

Organ and whole-body imaging

https://www.spectrum-dynamics.com/

Hybrid whole-body CZT imaging

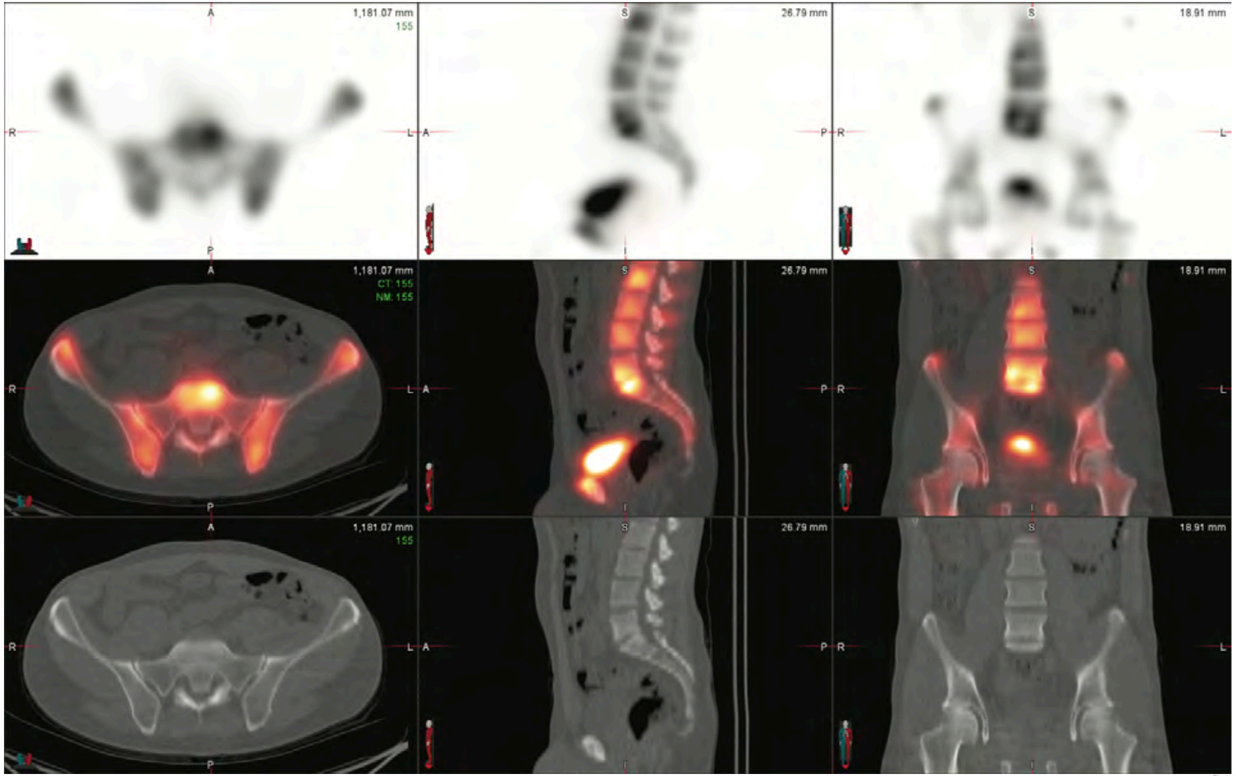

https://www.spectrum-dynamics.com/

Dedicated brain perfusion SPECT

G Model

ARTICLE IN PRESS

Available online at ScienceDirect

Elsevier Masson France EM|consulte www.em-consulte.com

ELSEVIER

Correspondence

Brain perfusion SPECT acquired using a dedicated brain configuration on a 360° whole-body CZT-camera

ARTICLE INFO

Keywords:
Brain perfusion
CZT
SPECT
Contrast
Spatial resolution
Image quality

Dear editor,

The development of whole-body cadmium zinc telluride (CZT) cameras contributes to recent advances in single photon emission computed tomography (SPECT) imaging, owing to high energy and spatial resolution of these CZT detectors [1]. These new type of cameras are now commercially available and have been so far studied for bone scintigraphy [2].

The Veriton-CT™ (Spectrum Dynamics Medical®) is a hybrid whole-body CZT-camera equipped with 12 swiveling high-resolution CZT detectors regularly spaced over 360 degrees. This system has the advantages of CZT detector features [1,3–5] and additionally benefits from 360° detector geometry which allows positioning of the detectors close to the patient's head and to focus the acquisition in a specific brain configuration (Fig. 1A).

An 81 year-old female presenting with neurocognitive impairment underwent brain perfusion SPECT acquisition [6,7] 15 minutes after a neurosensory resting period following the injection of 606 MBq of ^{99m}Technetium labelled-HMPAO [6] firstly with a conventional Anger-SPECT camera (Symbia T2™, Siemens Healthineers; parallel-hole collimators; 30-minutes acquisition) equipped with parallel-hole collimators and thereafter, with the Veriton™ CZT-camera, using the dedicated brain configuration (15-minutes acquisition). Axial slices of brain SPECT images obtained on both systems are presented in Fig. 1B and were optimized with a similar level of convergence of the iterative reconstruction process and CT slices (B) were used for further corrections of attenuation.

Tomographic count sensitivity was enhanced by a factor 2 with CZT as compared with Anger-SPECT (10.19 vs. 5.21 Mcounts/sec after decay correction) and signal-to-noise ratio was enhanced by a factor 1.5 (9.6 vs. 6.3) with CZT, measured within a homogeneous area centered on the semi-oval center. Spatial resolution and contrast of the CZT-SPECT images were also clearly enhanced, thus providing better visualization of the hypo-perfused areas associated with cortical atrophy (red arrows). It is likely that such improvements in both detection sensitivity and image quality will enhance the SPECT assessment of neurocognitive disorders [6], although this remains to be demonstrated by further dedicated studies.

To our acknowledgment, this is the first reported case of brain images obtained with a CZT-SPECT system, directly compared to a classical Anger-SPECT system. This distinct improvement in image quality, associated with a high potential for reducing acquisition time and/or injected activity, could support wider applications for brain perfusion SPECT studies, such as in ictal epileptic conditions [8] and for functional analyses of brain activation [9].

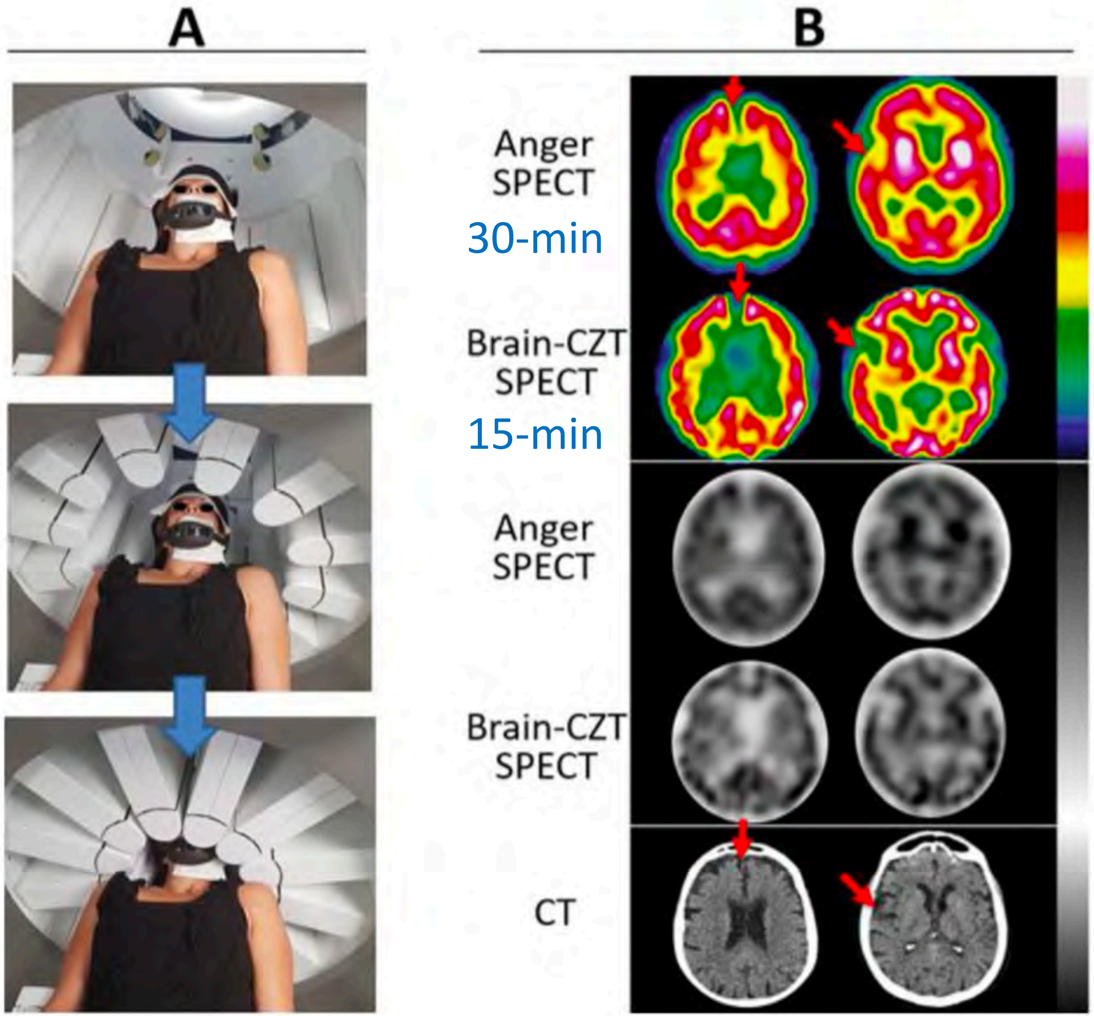

Improved image quality, potential to decrease activity or time

Bordonne M et al, J Neurorad 2019

Hybrid whole-body CZT imaging

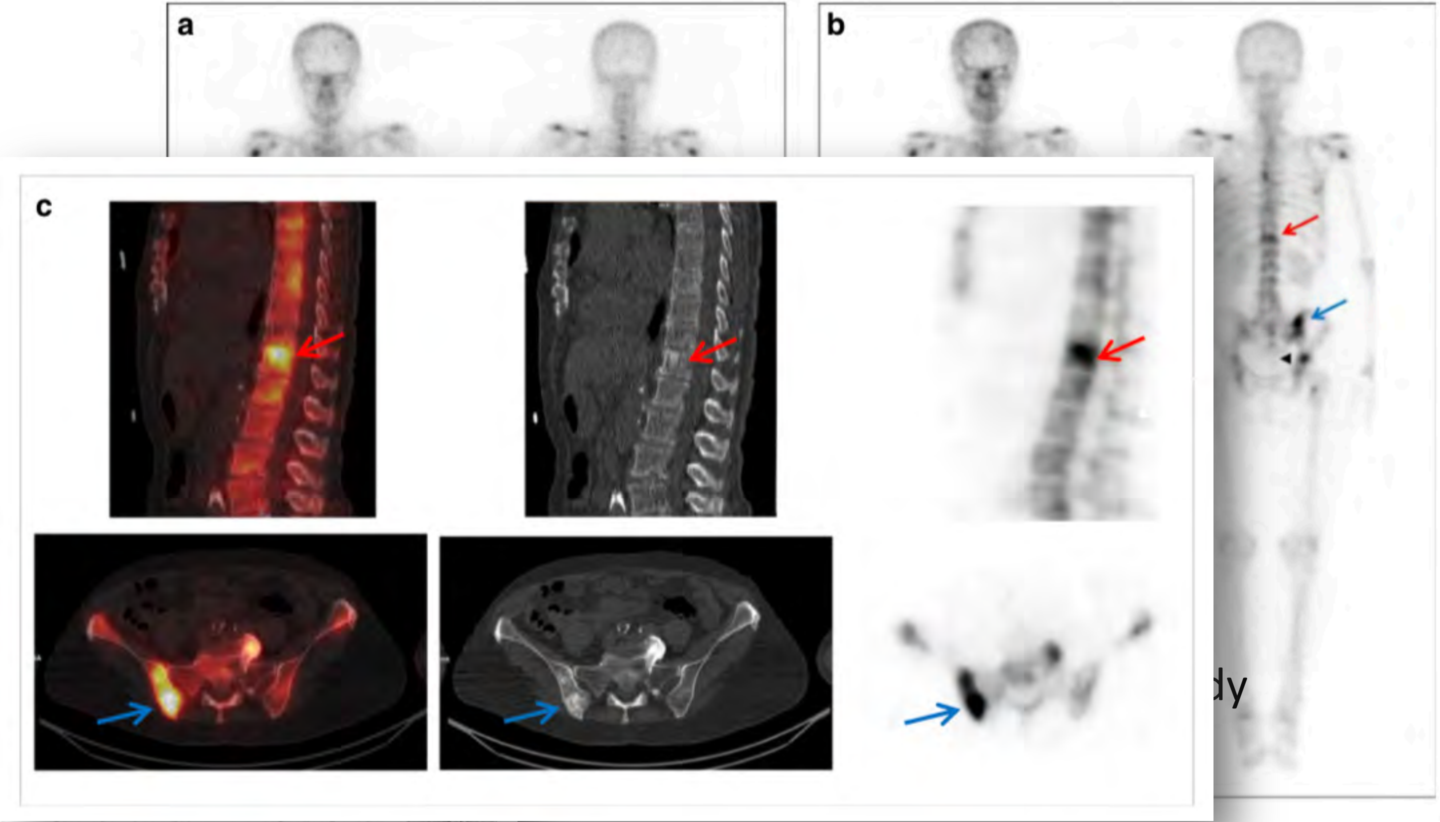

European Journal of Nuclear Medicine and Molecular Imag...
https://doi.org/10.1007/s00259-019-04525-y

IMAGE OF THE MONTH

Augmented planar bone scintigraphy obtained from a whole-body SPECT recording of less than 20 min with a high-sensitivity 360° CZT camera

Saifeddine Melki[1] · Mohammad Bilal Chawki[1,2] · Pierre-Yves Marie[1,3] · Laetitia Imbert[1,3,4] · Antoine Verger[1,3,4]

Received: 12 June 2019 / Accepted: 4 September 2019

Low-dose CT (<2 mSv)
(6 to 7) x (3-min bed position)

Melki S et al. EJNMMI 2019

SPECT/CT with GE 670 CZT

A Swiss experience

Courtesy of Renaud Guignard, MD, La Tour Hospital, Geneva, Switzerland

Cardiac MPI with hybrid whole-body, CZT-based camera

GE 670 CZT installed in June 2018, first 2 years: >800 MPI studies

Prone position (>75%), systematic gated-SPECT and (stress) CTAC

2 protocols:

– **1-day stress-rest** (90% of patients) with stress first and rest only performed if abnormal stress results

– **2-day stress-rest** for obese patients in screening setting (BMI > 35 kg/m^2)

Radiopharmaceutical: ^{99m}Tc-tetrofosmin

Pharmaceutical stress agent: regadenoson 400µg/5mL

Average total counts: 7 million counts (stress) / 25 million counts (rest)

Patient history:

- 68 year-old man; 123 kg (BMI 40.2)
- effort dyspnea; no history of CAD
- Negative pharmacologic stress test

Technical parameters:

- 1200 MBq ^{99m}Tc-tetrofosmin *(CT-scan DLP: 21 mGy.cm^{-1})*
- Supine position; 2 day-protocol

NAC

Stress-rest myocardial perfusion images *(NAC)*

QGS stress results

LVEF: 60%

EDV: 142 mL

ESV: 57 mL

QGS rest results

LVEF: 65%

EDV: 135 mL

ESV: 48 mL

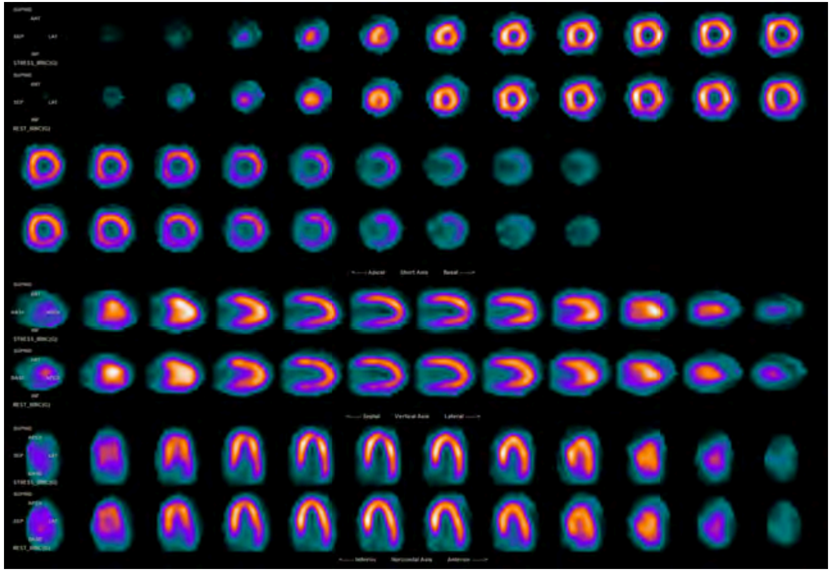

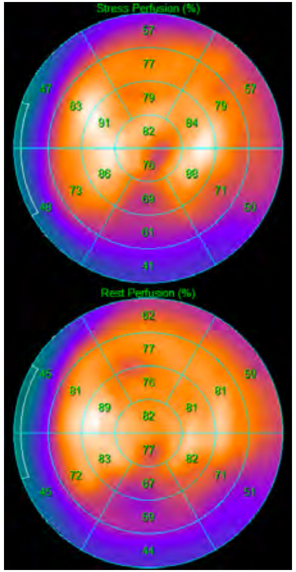

7.5-min

7.5-min

Decreased Acquisition Time by 30–40%

SPECT-CT acquisitions *(real time ≈ 10 minutes)*

30 x 2 projections; 15 secondes/bed

(L-configuration; 64x64; zoom 1.3; orbit:180°)

Reconstruction parameters:

OSEM 2it10sub; BW filter 0.4/10;+/- AC corrections

Patient history:

- 68 year-old man; 123 kg (BMI 40.2)
- effort dyspnea; no history of CAD
- Negative pharmacologic stress test

Technical parameters:

- 1200 MBq ^{99m}Tc-tetrofosmin *(CT-scan DLP: 21 mGy.cm^{-1})*
- Supine position; 2 day-protocol

Stress-rest myocardial perfusion images *(AC)*

AC

QGS stress results

LVEF: 60%

EDV: 142 mL

ESV: 57 mL

QGS rest results

LVEF: 65%

EDV: 135 mL

ESV: 48 mL

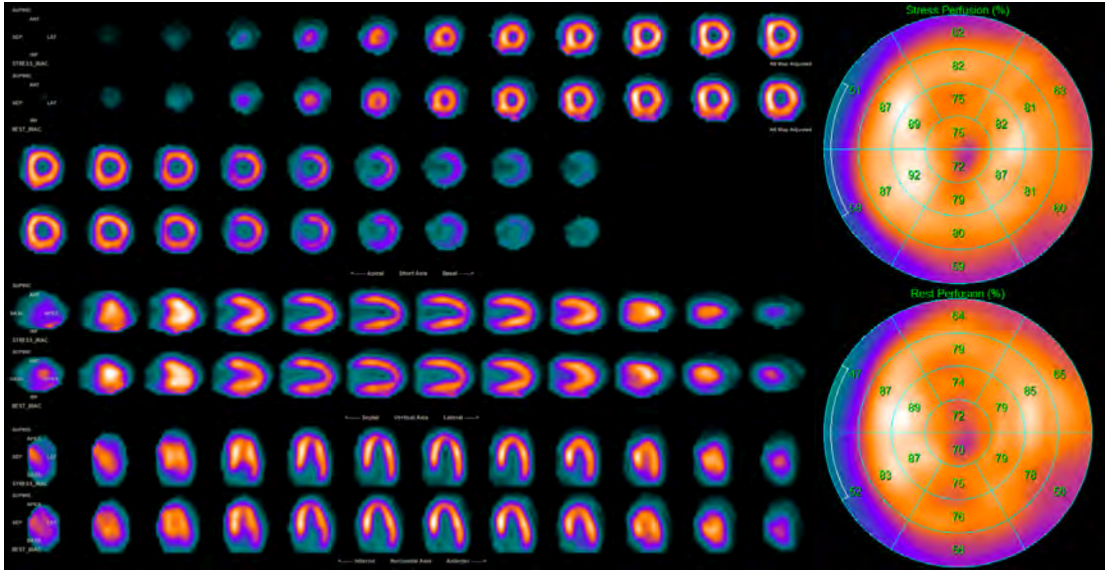

7.5-min

7.5-min

CONCLUSION

- No significative perfusion defect
- Inferior wall attenuation

SPECT-CT acquisitions *(real time ≈ 10 minutes)*

30 x 2 projections; 15 secondes/bed

(L-configuration; 64x64; zoom 1.3; orbit:180°)

Reconstruction parameters:

OSEM 2it10sub; BW filter 0.4/10;+/- AC corrections

La Tour Medical Group

Lung scan

No pulmonary embolism

Technical parameters:

- 80y old woman; 106 kg; BMI 41.1; supine position
- V: Technegas/ Q: 200 MBq ^{99m}Tc-MAA *(CT-scan DLP: 92 mGy.cm^{-1})*

VENTILATION (coronal AC view)

PERFUSION (coronal AC view)

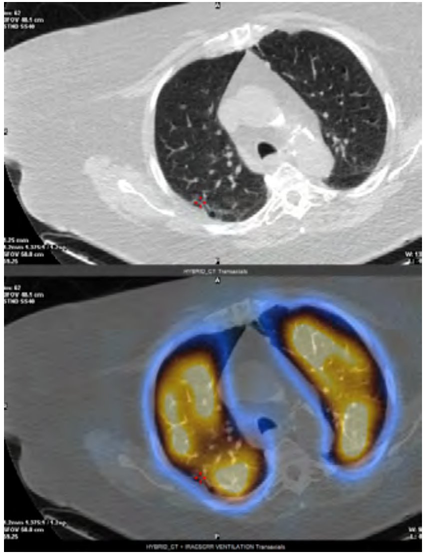

WB bone scan + 3FOV SPECT («PET-like») for oncological purpose

Technical parameters:

- 73y old man; 75 kg; BMI 29.3; supine position
- 781 MBq ^{99m}Tc-nanocolloïd *(CT-scan DLP: 620 mGy.cm^{-1})*
- Injection-acquisition time: 3 hours

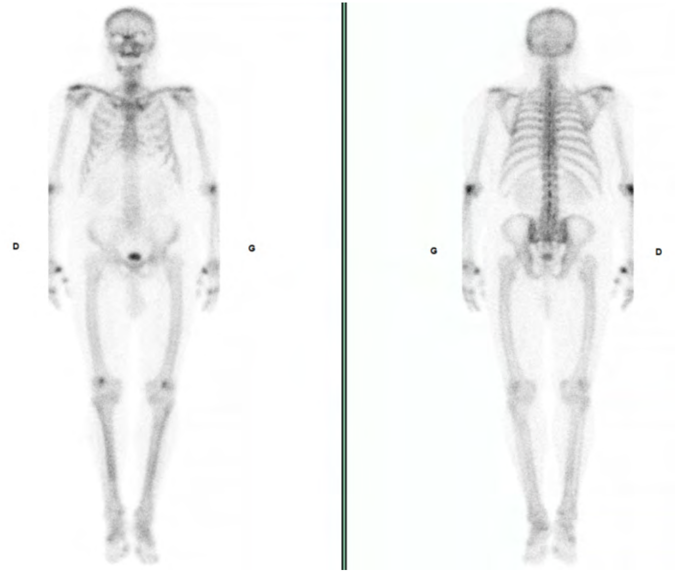

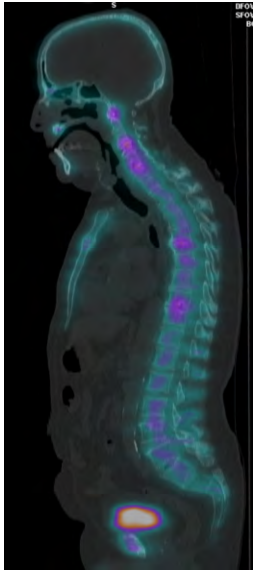

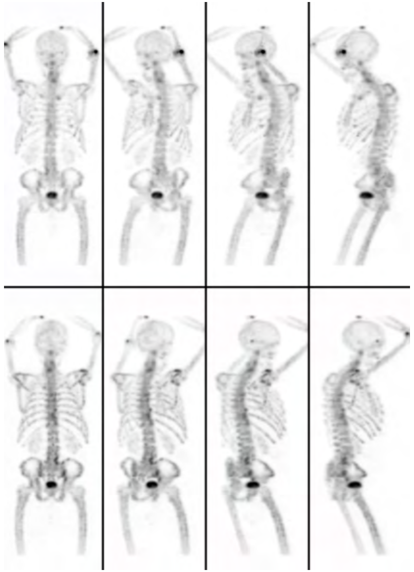

SPECT conclusion: no bone metastasis (initial staging of PCa; Gleason 9; PSA: 8 ng/mL))

La Tour Medical Group

DATscan *(+analysis)*

Technical parameters:

- 82y old man; 77 kg; BMI 23.8; supine position
- 191 MBq ^{123}I-Ioflupane
- Injection-acquisition time: 3 hours

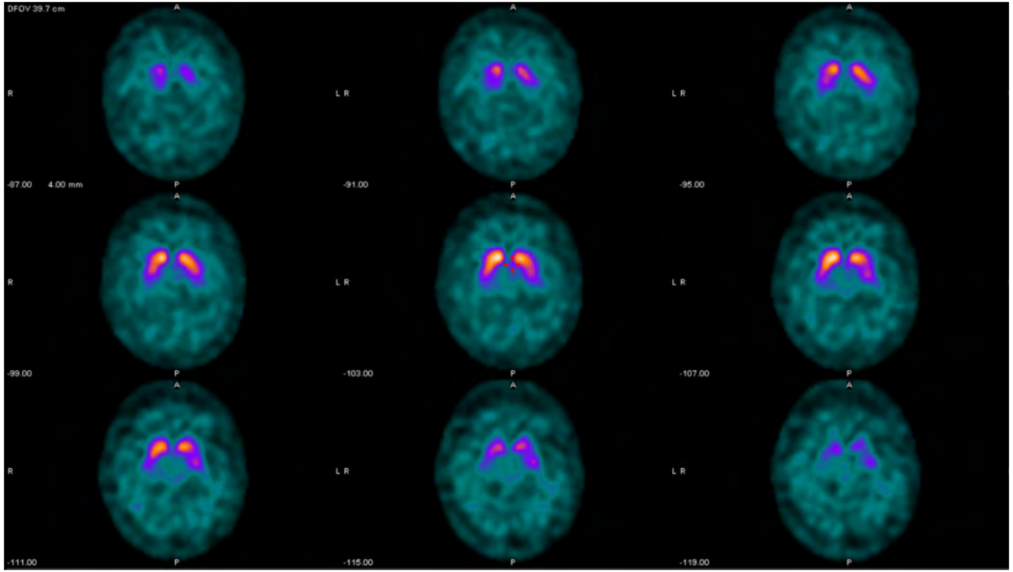

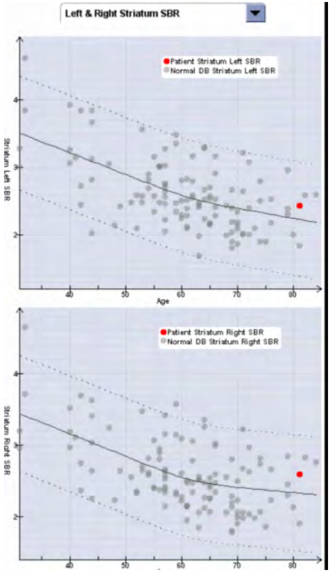

conclusion: normal exam

Unique dual-isotope simultaneous acquisition (CZT-improved energy resolution)

Cortical Region	Patient	Normal	Diff.	Z-Score
Prefrontal Lateral R	0.87	0.96	-0.09	-4.49
Prefrontal Lateral L	0.85	0.95	-0.11	-5.76
Prefrontal Medial R	0.84	0.95	-0.11	-3.53
Prefrontal Medial L	0.87	0.95	-0.07	-2.18
Sensorimotor R	0.98	0.94	0.03	1.26
Sensorimotor L	0.94	0.95	-0.00	-0.05
Anterior Cingulate R	0.85	0.93	-0.08	-1.53
Anterior Cingulate L	0.82	0.94	-0.12	-2.36
Posterior Cingulate R	1.01	0.99	0.02	0.54
Posterior Cingulate L	0.99	0.98	0.00	0.04
Precuneus R	1.13	1.00	0.13	3.99
Precuneus L	1.13	0.98	0.15	3.86
Parietal Superior R	0.99	0.91	0.08	1.92
Parietal Superior L	0.88	0.87	0.01	0.31
Parietal Inferior R	0.98	0.97	0.01	0.50
Parietal Inferior L	0.89	0.95	-0.06	-2.36
Occipital Lateral R	1.07	0.92	0.16	6.15
Occipital Lateral L	1.04	0.92	0.12	5.67
Primary Visual R	1.14	1.00	0.14	2.77
Primary Visual L	1.03	1.01	0.02	0.68
Temporal Lateral R	0.77	0.93	-0.16	-6.75
Temporal Lateral L	0.85	0.92	-0.07	-3.14
Temporal Mesial R	0.75	0.85	-0.10	-2.85
Temporal Mesial L	0.77	0.86	-0.09	-2.44
Cerebellum	0.95	0.93	0.02	0.69
Pons	0.83	0.87	-0.04	-0.70

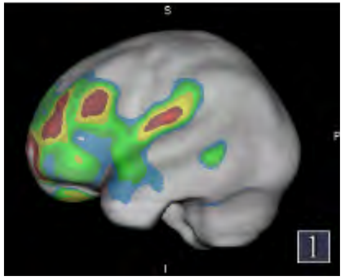

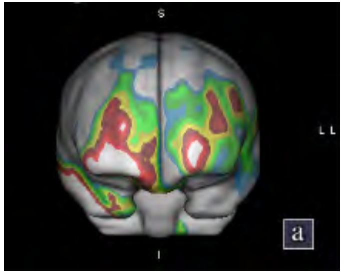

Ceretec™ & DATscan™

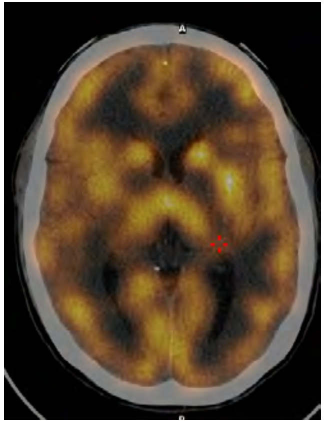

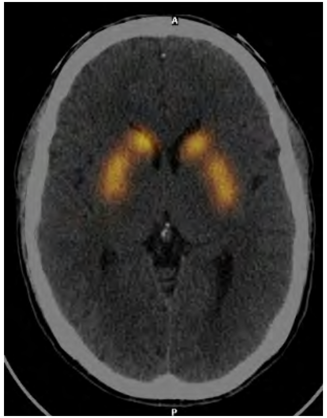

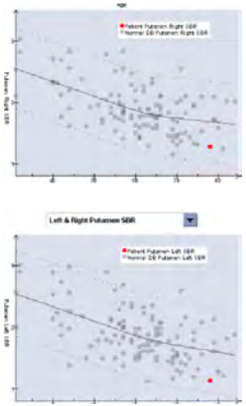

Comparison of whole-body vs. cardiac CZT

ORIGINAL ARTICLE

First comparison of performances between the new whole-body cadmium-zinc-telluride SPECT-CT camera and a dedicated cardiac CZT camera for myocardial perfusion imaging: Analysis of phantom and patients

Maxime Morelle, MD, PhD,[a] Dimitri Bellevre, MD,[b] Claude Hossein-Foucher, MD,[a] Alain Manrique, MD, PhD,[c,d] and Alban Bailliez, MD, PhD[b,c,e]

[a] Nuclear Medicine Department, Hôpital Roger Salengro, CHRU-Lille, Université de Lille 2, Lille, France
[b] Nuclear Medicine Department, IRIS, Hôpital Privé Le Bois, Lille, France
[c] Normandie Univ, UNICAEN, Signalisation, électrophysiologie et imagerie des lésions d'ischémie-reperfusion myocardique, FHU REMOD-VHF, Caen, France
[d] Nuclear Medicine, CHU de Caen, Caen, France
[e] Department of Nuclear Medicine, UF 5881, Groupement des Hôpitaux de l'Institut Catholique de Lille, Lomme, France

Received Jun 19, 2018; accepted Mar 11, 2019
doi:10.1007/s12350-019-01702-2

Background. Dedicated cardiac Cadmium-zinc-telluride (CZT) cameras show superior performances compared with Anger systems, particularly in terms of spatial resolution and count sensitivity. This study evaluated the performances of a new polyvalent whole body CZT camera (DNM 670CZT) compared with a cardiac dedicated CZT camera (DNM 530c) for myocardial perfusion SPECT.

Methods. The spatial resolution was evaluated with three linear sources filled with ^{99m}Tc. We used a cardiac phantom to evaluate count sensitivity, sharpness index, contrast-to-noise ratio, wall thickness, non-uniformity index, perfusion scores and ventricle volumes for both cameras. The impact of matrix size, and acquisition time was investigated. Concordance between the two cameras was evaluated in patients using QPS/QGS software for quantitative segmental perfusion, motion and thickness scores.

Results. The spatial resolution was identical with the two cameras. Count sensitivity of the DNM 670CZT was twofold lower compared with the DNM 530c, leading to lower sharpness index and contrast-to-noise ratio. The wall thickness and the myocardial volumes were similar. Visual and quantitative assessments of the perfusion patterns have shown a good concordance of the two cameras on phantoms and in patients.

Conclusion. This study demonstrated the feasibility of myocardial perfusion SPECT imaging using the new whole-body DNM 670CZT camera. (J Nucl Cardiol 2019)

Key Words: CZT-cameras • myocardial perfusion imaging • SPECT

- Acquisitions in phantom and N=10 patients
- Spatial resolution was identical
- Count sensitivity was 2x smaller with whole-body CZT with lower sharpness index and contrast-to-noise ratio
- Wall thickness and LV volumes were identical

Morell et al. JNC 2019

High-speed scanning of ^{123}I-mIBG planar images using a whole- body CZT camera

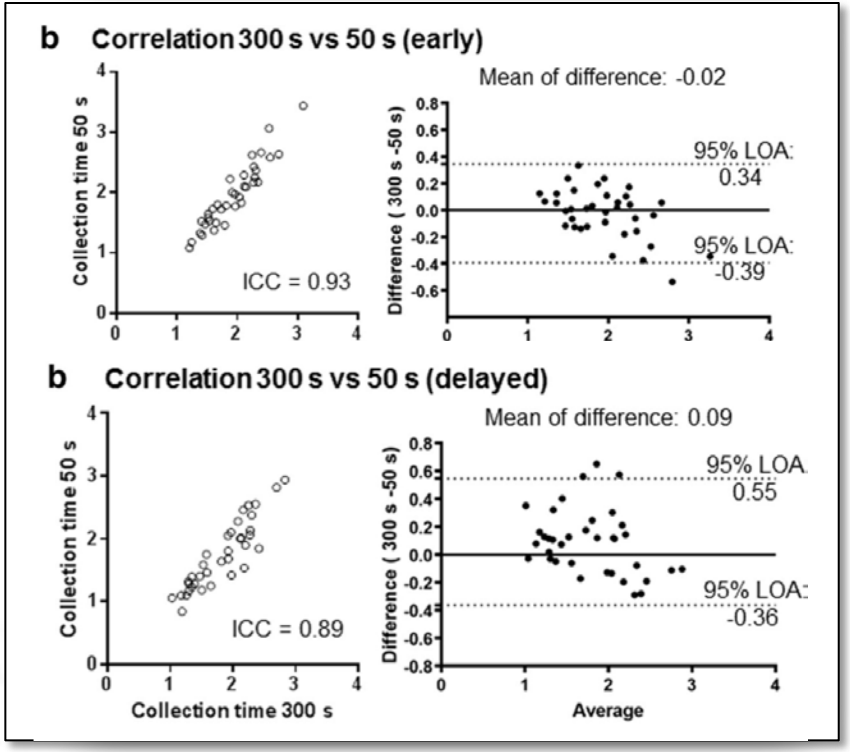

- N=36 patients
- List-mode acquisition
- Acquisition duration of 300-, 200-, 100- and 50-s
- →acquisition time can be reduced by 5x

Okano et al, EJNMMI Research 2019

Summary: Digital PET/SPECT Cameras

PET:

- Improved detectability & quantification in smaller structures, clinical impact++
- Lower injected activity AND scan duration
- Total-body PET: new horizons in systems biology imaging, high $$$
- 10-ps TOF PET Challenge: opportunity for even higher sensitivity (202X?)

SPECT:

- Increased energy resolution (2x better)
- Increased resolution as compared to conventional NaI camera
- Clinical impact less clear
- Lower scan duration OR less often decrease injected activity
- Only low-medium energy (no ^{131}I, not optimal for ^{111}In, ^{177}Lu)
- Electronic collimation (202X?)

Lausanne, Switzerland

Thank you for your attention!

http://the10ps-challenge.org